Kinetics-informed global assessment of mine tailings for CO_2 removal

Liam A. Bullock*, Aidong Yang, and Richard C. Darton

Department of Engineering Science, Parks Road, University of Oxford, Oxford, United Kingdom

*Corresponding author (liam.bullock@eng.ox.ac.uk)

Abstract

Chemically reactive mine tailings are a potential resource for drawing down carbon dioxide out of the atmosphere in mineral weathering schemes. Such carbon dioxide removal (CDR) systems, applied on a large scale, could help to meet internationally agreed targets for minimising climate change, but crucially we need to identify what materials could react fast enough to provide CDR at relevant climate change mitigation timescales. This study focuses on a range of silicate-dominated tailings, calculating their CDR potential from their chemical composition (specific capacity), estimated global production rates, and the speed of weathering under different reaction conditions. Tailings containing high abundances of olivine, serpentine and diopside show the highest CDR potential due to their favourable kinetics. We conclude that the most suitable tailings for CDR purposes are those associated with olivine dunites, diamond kimberlites, asbestos and talc serpentinites, Ni sulphides, and PGM layered mafic intrusions. We estimate the average annual global CDR potential of tailings weathered over the 70-year period 2030-2100 to be ~93 (unimproved conditions) to 465 (improved conditions) Mt/year.

Results indicate that at least 30 countries possess tailings materials that, under improved conditions, may offer a route for CDR which is not currently utilised within the mining industry. By 2100, the total cumulative CDR could reach some 33 $GtCO_2$, of which more than 60% is contributed by PGM tailings produced in Southern Africa, Russia, and North America. The global CDR potential could be increased by utilisation of historic tailings and implementing measures to further enhance chemical reaction rates. If practical considerations can be addressed and enhanced weathering rates

25 can be achieved, then CDR from suitable tailings could contribute significantly to national offset goals
26 and global targets. More research is needed to establish the potential and practicality of this
27 technology, including measurements of the mineral weathering kinetics under various conditions.

28 **Key words:** Enhanced weathering; Mine tailings; Mineral kinetics; Dissolution rates; Paris Agreement

29

30 **Highlights**

31 • Mine tailings host abundant silicate minerals that show high CDR potential
32 • Mineral dissolution kinetics are key to assessing potential of EW schemes
33 • Targeted enhanced weathering could speed up CO_2-water-tailings reactions
34 • Highly suitable chemically favourable tailings for CDR are globally distributed

35

36 **1. Introduction**

37 Increasing emissions of anthropogenic greenhouse gases and their link to global climate change (Field
38 and Raupach, 2004; Canadell et al., 2007; IPCC, 2018, 2019; Wilcox et al., 2021) suggest the necessity
39 for large-scale implementation of carbon dioxide removal (CDR) strategies. The scale envisaged is up
40 to 10 gigatonnes (Gt) CDR per year by 2050, rising to 20 Gt per year by 2100, if we are to meet the
41 Paris Agreement target of limiting global warming to well below 2°C this century (UNEP, 2017; NASEM,
42 2019; Wilcox et al., 2021). Clearly, the scale and novelty of such an undertaking call for urgent
43 improvement in our knowledge and methodological capabilities, to establish the societal and
44 engineering conditions required. Various methods of CDR are being actively investigated, including
45 the notion of utilising enhanced weathering (EW) of rocks and by-products of rock processing (e.g.,
46 Renforth and Henderson, 2017; Andrews and Taylor, 2019; Renforth, 2019; Beerling et al., 2020;
47 Darton and Yang, 2020; Bullock et al., 2021; James et al., 2021). The basic principle of the approach is
48 to rapidly react minerals with CO_2 to form stable hydrogen carbonate ions (bicarbonate or alkalinity;

Eqs. 1-2) or solid carbonate products (mineral carbonation; Eq. 3); these products can provide long term carbon storage, for hundreds of thousands of years (through alkalinity production) or millions of years (solid carbonate precipitates). The natural process, which EW aims to speed up, can be summarised as:

Carbonate rock and mineral weathering: $H_2CO_3 + CaCO_3 \rightarrow Ca^{2+} + 2HCO_3^-$ (1)

Silicate rock and mineral weathering: $2H_2CO_3 + CaSiO_3 \rightarrow Ca^{2+} + 2HCO_3^- + SiO_2 + H_2O$ (2)

Carbonate precipitation: $Ca^{2+} + 2HCO_3^- \rightarrow CO_2 + H_2O + CaCO_3$ (3)

When minerals are dissolved in these reactions with carbonic acid (Eqs. 1-2), divalent cations, which include Ca^{2+} (as shown in Eqs. 1-3) and Mg^{2+}, are released, stabilising the bicarbonates, and the products are transported to the ocean by rivers and are stored as alkalinity, or precipitate as carbonate minerals (Eq. 3). Both carbonate and silicate weathering reactions take CO_2 from the atmosphere, but as can be seen from Eq. (3), when bicarbonate precipitates as a carbonate, CO_2 is returned to the atmosphere, so that carbonate weathering followed by (secondary) precipitation provides no net removal of atmospheric CO_2. Alkalinity generation and carbonate production through weathering of silicate minerals is therefore the favoured route for net CDR.

In recent years, particular emphasis has been placed on mine tailings as a viable and voluminous source for CDR by alkalinity addition and secondary carbonate precipitation, due to their inherently favourable physical and chemical properties (Wilson et al., 2009a; Hitch et al., 2010; Pronost et al., 2011; Vogeli et al., 2011; Bodénan et al., 2014; Harrison et al., 2015; McCutcheon et al., 2016; Zarandi et al., 2016; Li et al., 2018; Kelemen et al., 2019; Power et al., 2020; Bullock et al., 2021). These properties include, but are not limited to, small grain sizes (typically sand sized or finer) and fresh (unweathered; previously unexposed to the atmosphere), high surface areas compared to in-situ rocks, with high production tonnages of Ca- and Mg-rich silicate minerals also available (Bullock et al., 2021). The key advantage of mine tailings is that favourable material conditions and high

tonnages are available through conventional mining: further processing, such as costly grinding to make smaller particles, may not be necessary. Several studies have identified specific mine tailings likely to be favourable for CO_2-water-rock reactions, mineral dissolution, and secondary precipitation. For instance, Ni sulphide deposits (e.g., Assima et al., 2014; Wilson et al., 2014; Power et al., 2020), asbestos mines (e.g., McCutcheon et al., 2016, 2017), and kimberlite-hosting diamond mines (e.g., Wilson et al., 2009b; Mervine et al., 2018) have been highlighted because the fast-reacting Mg-hydroxide mineral brucite occurs in the tailings. However, brucite is not universally present in mafic and ultramafic rocks, and where it does occur, it is usually in low volumetric abundance. As a result, a recent study by Bullock et al. (2021) also emphasised the role of silicate-rich mine tailings, which could potentially capture substantial amounts of CO_2 if conditions were optimised. The study of Bullock et al. (2021) presents an example calculation showing the importance of mineral kinetics for CDR, but does not explore this further. A detailed assessment of mineral kinetics for CDR is important, however. Many minerals simply do not react fast enough to contribute significant CDR by the target dates of 2050 and 2100. When assessing the potential of mineral resources, it is necessary to check that the weathering (dissolution) rates are sufficient to provide CDR on decadal timescales.

Silicate minerals such as olivine, serpentine, wollastonite, enstatite, and diopside show some potential for CDR by alkalinity addition and mineral carbonation (Schuiling and Krijgsman, 2006; ten Berge et al., 2012; Dudhaiya et al., 2019; Haque et al., 2019; Bullock et al., 2021). These minerals commonly accumulate as unwanted waste material in a range of mine tailings, such as those associated with metallic, diamond, and refractory mineral mining operations, a wider range of potentially viable tailings materials for CDR purposes than is currently being investigated. These materials also have a global coverage, and some regions may host voluminous resources that are currently overlooked for CDR purposes. Countries and regions that have already been studied for their overall CDR potential by alkalinity addition and mineral carbonation include the United States (Krevor et al., 2009), United Kingdom (Renforth, 2012), Japan (Myers and Nakagaki, 2020), and South Africa (Hietkamp et al., 2004; Vogeli et al., 2011; Meyer et al., 2014). However, there is a need for a wider

global identification of suitable tailings materials, their properties (including weathering rates), and their CDR potential.

This study presents a global and national-level assessment of the suitability of different tailings materials for CDR purposes. Our approach goes further than previous studies by considering the impact of mineral weathering kinetics on CDR, enabling us to target resources which can contribute to achieving climate goals in this century. We assess tailings materials in terms of chemistry, production tonnages and reaction kinetics. This knowledge informs selection of locations and mine sites where relevant issues of dissolution and precipitation, space and energy requirements, and other information key to assessing large scale deployment can be addressed. Focusing on the implementation time window of 2030-2100, our objectives are to indicate where opportunities for CDR with tailings exist and the potential magnitude of carbon capture. We examine the premise that utilising mine tailings for CDR could help some individual countries achieve their own CO_2 offset goals, as well as contributing to the CDR required to achieve Paris Agreement targets for limiting global warming.

2. Methodologies

2.1. Initial list of assessed mine tailings

To estimate the total global CDR potential of mine tailings, and identify the countries where the highest potential exists, materials have been ranked based on their overall CDR suitability. This ranking is based on (1) the maximum chemical potential for alkalinity addition and mineral carbonation, (2) the annual volumetric production tonnages, and (3) the modal abundances of kinetically favourable minerals and timescales of mineral dissolution. Any materials that show promising results for these three properties are considered here as suitable for CDR purposes. In Bullock et al. (2021), and in this study, *chemical favourability* of a mineral or material means that it has the capacity to react with CO_2

through the appropriate chemistry; commonly this involves materials with high CaO or MgO content, or with high modal abundance of Ca- or Mg-bearing minerals. A mineral which shows promising reaction rates on relevant timescales is considered here to have *kinetic favourability* (see section 2.2).

The initial list of tailings materials to be assessed (Table 1) was taken from the study of Bullock et al. (2021), which provides the most comprehensive survey of silicate-hosted mine tailings for CDR purposes to date. These materials were chosen because they are the main silicate-dominated tailings types produced from metal, diamond, and mineral commodity extraction, offering high amounts of MgO and CaO due to high Ca- and Mg-silicate targetable mineral contents (Supplementary Table A). Previous work by Bullock et al. (2021) provided an indicator of CDR suitability based on material chemistry ("E_{pot}"; see also Renforth, 2019). These E_{pot} values describe the maximum hypothetical CDR specific capacity of a given material, through alkalinity production, assuming 100% mobility of fluid soluble cations, but with no detailed account taken of reaction kinetics and timescales of mineral dissolution. The E_{pot} values (measured in $kgCO_2/t$, or gCO_2/kg) were calculated for tailings materials using their bulk mineral contents based on the whole rock compositions taken from literature examples. The E_{pot} value was calculated using the formula of Bullock et al. (2021), a modified version of the formulae described in Renforth (2019), and based on Steinour (1959) (Eq. 4):

$$E_{pot} = \frac{M_{CO_2}}{100} \cdot \left(\alpha \frac{CaO}{M_{CaO}} + \beta \frac{MgO}{M_{MgO}} + \varepsilon \frac{Na_2O}{M_{Na_2O}} + \theta \frac{K_2O}{M_{K_2O}} + \rho \frac{MnO}{M_{MnO}} + \gamma \frac{SO_3}{M_{SO_3}} + \delta \frac{P_2O_5}{M_{P_2O_5}} \right) \cdot 10^3 \cdot \eta \quad (4)$$

The coefficients α, β, γ, δ, ε, ρ, and θ, which consider the relative contribution of each oxide to CDR (see Renforth, 2019) were adjusted based on the modal carbonate content of the rock (see Bullock et al. (2021), as carbonate weathering has a lower CDR capacity than silicate weathering. Mineral carbonation potential (C_{pot}), where bicarbonate products precipitate as carbonate minerals, may also be calculated for CDR potential including this (secondary) precipitation of carbonates (Eq. 5):

$$C_{pot} = \frac{M_{CO_2}}{100} \cdot (\alpha * \frac{CaO}{M_{CaO}} + \beta \frac{MgO}{M_{MgO}} + \gamma \frac{SO_3}{M_{SO_3}} + \delta \frac{P_2O_5}{M_{P_2O_5}}) \cdot 10^3 \quad (5)$$

In Eqs. 4-5, elemental concentrations of the materials are expressed as major element (wt%) oxides, M_x is the molecular mass of those oxides, and η is molar ratio of CO_2 to cation sequestered during weathering. For silicate minerals, η = 1.5 to account for buffering in the seawater carbonate system (Renforth and Henderson, 2017; Renforth, 2019; Bullock et al., 2021). See Renforth (2019) and Bullock et al. (2021) for full details of the methodology.

Available tonnages of suitable tailings materials were calculated based on the targeted commodity production tonnages for the year 2020 (taken from U.S. Geological Survey mineral commodity summaries; USGS, 2021). For these tonnages, the proportional contribution of annual production of each commodity from different host rocks (e.g., diamond production from kimberlites, Ni production from Ni sulphides etc) has been estimated based on information presented in Kesler and Simon (2015), Ndlovu et al. (2017) and USGS (2021). Tailings volumes were calculated based on known ratios of commodity production to tailings production from cited global examples (see Supplementary Material B). Mean, maximum, and minimum tailings production tonnages reflect the mean, maximum, and minimum conversion factors of commodity production to tailings production from the global examples. For estimates of 2030 production commodity (and subsequent tailings) tonnages, the anticipated commodity market growth was also added to the 2020 production volume examples (see Supplementary Material B). Estimates of market changes from 2030 to 2100 are generally lacking, thus annual tailings production projections were kept constant from 2030 onwards, i.e., annual production is kept at the same value for the period 2030-2100. In practice demand and production will fluctuate, with changes in commodity demand, extraction efficiency, and efforts to reduce non-essential mining activities and waste production. However, such changes are difficult to predict, and our constant value provides a defined base case.

2.2. Mineral kinetics

Mineral dissolution kinetics are assessed as part of the overall determination of tailings material suitability. We use published dissolution rates (under various initial reaction conditions) based on the release of silicon which holds together the mineral framework (Oelkers, 2001) (denoted as W_r; see compilations of Palandri and Kharaka, 2004; Bandstra et al., 2008, and Supplementary Table B).

As a guide to which minerals have a sufficiently fast weathering rate to be considered kinetically favourable, a baseline W_r has been established. Qualitatively, the rates achieved for olivine dissolution (specifically for the more Mg-rich end member forsterite) could be viewed as a baseline, as it has been recognised as a mineral with high potential for CDR (e.g., Giammar et al., 2005; Hänchen et al., 2006; Hangx and Spiers, 2009; Schuiling and de Boer, 2011; Wang and Giammar, 2013; Rigopoulos et al., 2015). Olivine's weathering rate, under near-neutral pH conditions and ambient temperatures, is, on average, ~$10^{-10.1}$ mol/m^2/s, typically ranging ~$10^{-9.6}$ to $10^{-10.6}$ mol/m^2/s based on compiled published results (e.g., Wogelius and Walther, 1992; Pokrovsky and Schott, 2000; Palandri and Kharaka, 2004; Bandstra et al., 2008).

An alternative approach to establishing a baseline is to estimate dissolution times, for example with a shrinking core model such as used by Renforth et al. (2015) and Kelemen et al. (2020). This provides an estimate for the near-complete (90% reaction) dissolution time of common rock-forming minerals at a range of mean particle sizes. For typical tailings grainsizes of 50-100 μm (Supplementary Table A), relatively fast mineral dissolution rates of greater than ~$10^{-10.5}$ mol/m^2/s are required for near complete weathering of minerals on timescales of years to decades, based on the model of Kelemen et al. (2020). This rate is in fact close to that typical of olivine (Palandri and Kharaka, 2004; Bandstra et al., 2008), and was thus taken as a guideline to target the most viable Ca- and Mg-bearing silicate minerals.

As the aim of EW is to speed up reaction rates of minerals for CDR, minerals which are reported as up to 2 orders of magnitude lower than the baseline rate are considered to be potential targets. This range was chosen to allow for the possibility that weathering rates might perhaps be

195 "improved" (increased) by a factor 10-100 through implementing different EW methods (see
196 Discussion). We require a rate of ~$10^{-10.5}$ mol/m^2/s for near complete weathering on decadal
197 timescales, so our baseline limit for screening purposes is W_r of ~$10^{-12.5}$ mol/m^2/s. If a tailings resource
198 demonstrates a weathering rate greater than this value, it is considered as "kinetically favourable" for
199 CDR.

200 The tailings material kinetics were evaluated based on their typical modal mineralogies
201 (Supplementary Tables A-C) and the average published W_r of each targeted mineral (Table 2 and
202 Supplementary Table B). A theoretical 1 kg of each tailings material of a typical modal mineralogy
203 (after Bullock et al., 2021) has been considered using a shrinking core model (after Renforth et al.,
204 2015), where the modal mineralogy is converted to grams of mineral in the tailings, with untargeted
205 minerals (e.g., pyrite, magnetite, apatite) excluded from calculations, leaving only the targetable
206 minerals. The model is used to determine the CDR capacity of each mineral phase within the given 1
207 kg of tailings, and the sum for all mineral phases in the sample then gives the overall potential of the
208 material. The shrinking core model used here is:

209 $$X(t) = \frac{D_0^3 - (D_0 - 2W_r V_m t)^3}{D_0^3} \qquad (6)$$

210 Where X is the fractional extent of dissolution, t is dissolution time (s), D_0 is the initial particle diameter
211 (m; converted from a typical grain size for each tailings type (μm), shown in Supplementary Table B),
212 W_r is the average dissolution rate from literature examples (mol(mineral)/m^2/s), and V_m is the molar
213 volume of the mineral (m^3/mole, converted to one mol Si basis). Published W_r values were taken from
214 experimental studies, allowing for processes such as secondary (non-carbonate) precipitation,
215 agglomeration, and/or silica surface passivation, which can act to hinder W_r. Calculations were first
216 made for published W_r achieved at near-neutral pH (~6-8) solution and ambient temperatures (21-
217 24°C), here classified as "unimproved" reaction conditions, as the intention is to permit reactions to
218 take place without deliberate efforts to enhance reaction rates. Calculations were then made for the

same 1 kg of materials under "improved" conditions, whereby grain size was reduced to a single lower limit particle size of 10 μm for all tailings types (a size utilised in other EW studies, e.g., Beerling et al., 2020), and pH was notionally reduced to more acidic conditions by using, in the shrinking core model, published W_r values achieved at pH 3-4. Improved conditions are a deliberate attempt to increase reaction rates using controlled or engineered methods to achieve enhanced weathering conditions and increased dissolution rates compared to those achieved in natural "unimproved" settings.

2.3. Tailings material kinetics and calculation of CDR trajectory

Materials were initially modelled based on an assumed average grain size (published examples, see Table 2, Supplementary Material A and Supplementary Tables A and C), with a range of published W_r (Supplementary Table B) used to highlight the differences in CDR rates under different starting conditions, as well as the inherent uncertainty associated with each mineral and consequently each tailings material. The extent of dissolution, as a percentage and in grams, and the overall CDR of each theoretical 1 kg of material, were assessed on Paris Agreement-relevant timescales of 1 year up to 70 years (e.g., reflective of reactions for the operational period 2030-2100). For each run and scenario (under unimproved and improved conditions), an estimate of dissolution over a given period of time is found for each mineral present in the theoretical 1 kg. Cumulative CDR potential due to alkalinity (Eq. 2) of 1 kg of tailing *i* for a time duration *t*, referred to below as specific CDR (*s*CDR), can be calculated by:

$$sCDR_i(t) = \sum_j f_{i,j} X_{i,j}(t) E_{pot}^{j} \qquad (7)$$

where $f_{i,j}$ is the mass fraction of mineral *j* in tailings *i*, $X_{i,j}$ is the extent of dissolution calculated using the shrinking core model (Eq. 6) using the kinetics of mineral *j* and the initial particle size of tailing *i*, and E_{pot}^{j} is the E_{pot} for mineral *j*.

Considering the implementation time window from year 2030 to year 2100 using freshly produced tailings each year in this period, the total cumulative CDR (referred to as *t*CDR) of tailing *i* by a particular year *y* in this period, which includes the cumulative contribution from the tailing produced in all the years (*k*) up to and including year *y*, can be calculated by:

$$tCDR_i(y) = \sum_{k=1}^{y} sCDR_i(t_k) P_{i,k} \quad (8)$$

where t_k is the time elapsed from year *k* to year *y*, and $P_{i,k}$ is the mass of tailing *i* produced in year *k*, with *k* = 1 denoting the year 2030. Depending on the geographical region considered, $P_{i,k}$ may represent the tailings output either of a country or globally. The CDR achieved annually (referred to as *a*CDR) of tailing *i* in year *y* can then be simply derived:

$$aCDR_i(y) = tCDR_i(y) - tCDR_i(y-1) \quad (9)$$

Finally, aggregating total cumulative (*t*CDR) or annual (*a*CDR) CDR values of all the tailings considered yields what mine tailings as a whole could offer in a country or worldwide. Using national commodity production estimates of USGS (2021), and following the same production estimate method procedure as outlined in section 2.1, the CDR potential of each suitable tailings-hosting country was calculated for a nation-by-nation assessment. Estimates were made for each country for the year 2030, and the cumulative totals (*t*CDR) by 2050 and 2100.

For a particular geographical area, the cumulative mass of tailings i produced over y years is M_i, where:

$$M_i = \sum_{k=1}^{y} P_{i,k} \quad (10)$$

For these tailings, the CDR potential due to alkalinity per unit of materials supplied to an EW scheme during a specified period of operation is therefore:

$$E_{pot}^{op,i}(y) = \frac{tCDR_i(y)}{M_i} \quad (11)$$

Eqs. (6) to (11) are employed to estimate the CDR potential of a tailings type by producing alkalinity (i.e., based on E_{pot}), on the time scale of interest for mitigating climate change, the duration y years. A similar set of equations can be applied on the basis of C_{pot}, leading to the calculation of $\mathrm{C}_{pot}^{op,i}$, the CDR potential of converting tailing *i* to carbonate products per unit of materials supplied to an EW scheme during a specified period of operation. Calculation of $\mathrm{E}_{pot}^{op,i}$ and $\mathrm{C}_{pot}^{op,i}$ requires knowledge of the following tailings characteristics: mineral composition of the tailings; chemical composition of each mineral present; initial grain size; dissolution (weathering) rate W_r; production profile for the tailings for the period y years.

3. Results

3.1. Targetable minerals

Based on the published W_r and desired baseline rate (here, ~$10^{-12.5}$ mol/m^2/s), targetable Ca- and Mg-bearing silicate minerals include wollastonite, olivine (Mg-rich forsteritic end member), amphibole (hornblende), serpentine group minerals (lizardite and chrysotile), orthopyroxene, clinopyroxene, plagioclase, talc, biotite mica, and chlorite (clinochlore) (Table 2). Wollastonite, olivine, and diopside (clinopyroxene end member) show the highest W_r, comparable to the desired baseline rate. These minerals have been previously studied for their CDR potential, warranting their inclusion, for instance, olivine (e.g., Hänchen et al., 2006; Hangx and Spiers, 2009; Schuiling and de Boer, 2011; ten Berge et al., 2012), wollastonite (e.g., Dudhaiya et al., 2019; Haque et al., 2019) and pyroxene group minerals (e.g., Rigopoulos et al., 2015). Serpentine-rich rocks have also been identified as viable CDR materials (e.g., Krevor et al., 2011; Oskierski et al., 2013; Lacinska et al., 2017), as serpentine is commonly formed by alteration of peridotite, an igneous rock mainly comprised of olivine and pyroxene. Beyond those minerals previously studied for CDR purposes, other pyroxene and plagioclase group minerals also meet the baseline rate (Table 2). The inclusion of the broader pyroxene and plagioclase groups as

targetable minerals comes with the added advantage that these two mineral groups are prominent in many tailings materials, with potentially vast amounts of material available for CDR schemes (see typical modal mineralogies in Supplementary Table A). Chlorite and talc weathering rates also meet the baseline value; though data is limited for these minerals, their composition suggests that they could be promising CDR candidates, and they are therefore included in this study.

3.2. Determination of most suitable tailings for CDR

Suitable tailings are those that show promising whole rock chemical potential (E_{pot} and C_{pot} based on their typical bulk rock geochemistry), significant production tonnages, and/or contain a majority modal mineralogy of the targetable minerals shown in Table 2, and identified in section 3.1. The list of tailings materials for further assessment, based on their modal mineralogies (e.g., >50% targetable minerals) and whole rock E_{pot} (e.g., >100 gCO_2/kg), includes asbestos and talc serpentinites, Cr layered intrusions and podiforms, Cu porphyry and VMS deposits, diamond kimberlites, Ni sulphides, olivine dunites, Pb-Zn skarns, PGM layered mafic intrusions, and Ti anorthosite deposits. Commodity-holding host rocks and their associated tailings by-products ("deposit types") were assessed by Bullock et al. (2021) based on their volumetric abundance and their chemical favourability, but reaction kinetics were only considered for one theoretical example. In the present study, it became clear that some of the materials assessed in the previous study do not show the right kinetic favourability to be effective on timescales relevant to climate mitigation (slow weathering kinetics) or are almost entirely comprised of minerals unreactive for CDR purposes, generally lacking Ca- and Mg-rich components.

Of the 31 different tailings materials assessed here, 12 show high (>50%) modal abundances of targetable minerals, and mean E_{pot} values greater than 100 gCO_2/kg tailings material, warranting further consideration for CDR purposes (Table 3). These include Ni sulphides, dunites, serpentinites, kimberlites, skarns, and layered mafic intrusions, which in general contain >70% of targetable minerals. Some of these materials have been previously studied for their CDR potential, e.g.,

serpentinites (McCutcheon et al., 2016, 2017) and Ni sulphide deposits (Wilson et al., 2014; Power et al., 2020), with more limited attention paid to kimberlites (Wilson et al., 2009b; Mervine et al., 2018), olivine-rich dunites (Kremer et al., 2019), and layered mafic intrusions (Vogeli et al., 2011; Meyer et al., 2014). Some Cu and Ti deposits, which occur in economic concentrations across a wide range of geological settings, contain >50% of these targetable minerals, such as those derived from more mafic host rocks. These specific host rock types and associated tailings are therefore assessed here. Cu mine tailings are also amongst the most volumetrically abundant that are produced annually (>2 Gt/year; Bullock et al., 2021), so they could prove a significant CDR material. Based on the E_{pot} and C_{pot} values shown in Supplementary Table A, Pb-Zn-hosting skarn deposits show a high potential for CDR, comparable to the previously studied materials discussed above: skarns sometimes contain high amounts of targetable minerals such as pyroxene, plagioclase, and amphibole, as well as minor wollastonite content.

Other materials, such as Cu IOGC, Cu sediment-hosted deposits, and Fe-hosting Kiruna-type deposits, may show similar chemical favourability (E_{pot} values). These may contain general modal mineralogies akin to Cu mafic porphyry/VMS deposits, and Ti anorthosite deposits, though their mineralogy is generally less variable. The majority of IOGC, sediment-hosted, and Kiruna-type deposits will contain more Ca-Mg-deficient and more kinetically inhibited minerals such as quartz, some clays, and Fe-oxides, so these materials are excluded from further assessment. Tailings from Fe, Sn, and U mining operations are large in volume (Bullock et al., 2021), but their chemical favourability is generally low, so they are unsuitable for CDR and are excluded from further consideration.

3.3. Mineral and material kinetics

Dissolution times and CDR potential (*s*CDR) of the assessed tailings materials under unimproved reaction conditions are shown in Table 3. “Unimproved reaction conditions” are taken as (a) initial particle size is the typical reported mean grain size of each tailings material (see Supplementary Table

A and Supplementary Material A), and (b) weathering rate is the average published W_r value achieved at near-neutral (pH 6-8) solution reaction conditions at temperature 21-24°C.

The results show, as anticipated, that tailings containing higher abundance of olivine are generally more kinetically favourable than olivine-poor or olivine-absent materials, with higher *s*CDR and higher overall dissolution extent often achievable within decadal to centennial timescales. Depending on the initial grain size, olivine dissolution extent of 0.3-1% is achievable in one year, and ~20-55% over 70 years (Table 3). Olivine-rich tailings also show a greater potential to reach their maximum E_{pot}, particularly at the higher published W_r values. Based on maximum W_r values, serpentine may undergo full dissolution within 70 years. Serpentine and plagioclase show a wider range of W_r values so that, in many cases, their dissolution extent over a given time and *s*CDR capacity varies from highly promising, reaching their E_{pot} capacity in decadal timescales, to low, taking millenia to millions of years to undergo full dissolution. This huge range is in part due to the variability of published W_r values for different plagioclase and serpentine end members. Evidently there is a great degree of uncertainty associated with plagioclase and serpentine-rich tailings. Finally, we note the importance of average grain size; finer grained materials of the same mineralogy can be several orders of magnitude faster in undergoing dissolution. Accordingly, tailings that are more finely ground in conventional processing (e.g., typically 75 µm in diameter or mean grain size for PGM, diamond, and asbestos extraction) have an advantage over those that are coarser (e.g., 100-250 µm for Cr, Ni, Cu, and Ti extraction) under unimproved reaction conditions (i.e., with no additional EW processes applied).

Olivine dunite tailings show the highest CDR kinetic ranking, based on the highest average calculations (*s*CDR of ~371 gCO_2/kg tailings by alkalinity after 70 years of weathering; Table 3), and the greatest amount of CDR (123-757 gCO_2/kg tailings by alkalinity production after 70 years; maximum and minimum values reflect the different published W_r values under unimproved conditions). The addition of a carbonation step, whereby CO_2 is removed through weathering followed by carbonate

precipitation, would reduce the CDR by about 56% on average across tailings materials (calculations based on C_{pot} values of minerals rather than E_{pot} values). Following olivine dunite, there is a cluster of tailings materials that show between (on average) ~55-120 g *s*CDR per 1 kg of material after 70 years through alkalinity production. This cluster includes diamond kimberlite tailings having the second highest average CDR, down to PGM layered mafic intrusion tailings which have about half the specific CDR potential of diamond kimberlite.

Other tailing types have notably lower *s*CDR values than the PGM tailings group. Tailings associated with Cu, Cr, Ti, and Pb-Zn deposits are typically below 55 g *s*CDR average after 70 years, the upper value representing Cr podiform deposits. While Cr podiform tailings show some potential for CDR, layered intrusion-derived Cr tailings are much lower (<1 gCO_2/kg). Mineralogically, Cr layered deposits can be closely associated with PGM layered mafic intrusions and Cr podiforms, suggesting that their overall CDR potential may be higher than estimated here. Similarly, tailings associated with Cu porphyry and VMS, Ti anorthosite and Pb-Zn skarn deposits can also contain more kinetically favourable minerals such as olivine, serpentine, and wollastonite. Therefore, Cu, Cr, Ti, and Pb-Zn tailings are not completely ruled out for CDR purposes, but their mineralogy requires more research, perhaps for CDR schemes on a more regional geological basis. The high global tonnage of Cu tailings means that, even if only a small percentage of materials are kinetically favourable, these could still be considered as lucrative CDR targets. However, we conclude that, if chemical favourability, mineral kinetics and production tonnages are all considered, the most suitable tailings targets for CDR purposes are those associated with asbestos and talc serpentinite deposits, diamond kimberlites, Ni sulphide deposits, olivine dunites, and PGM layered mafic intrusions (Figs. 1-3 and Supplementary Fig. A).

3.4. Global and national-level CDR

By focusing on only the most suitable tailings materials, it is possible to identify the most attractive mine-hosting countries for CDR, particularly when using improved EW schemes (Fig. 4 and Supplementary Figs. A-C). All commodities that are responsible for the production of suitable tailings are anticipated to show annual market growth between 2020 and 2030 (see Supplementary Material B). If concentration and tailings production technologies remain relatively constant in terms of production efficiency through this period, the amount of tailings associated with these commodities will also rise. Market growth of ~2-5% across these commodities has been forecast, with the nickel and PGM commodity markets perhaps achieving a 5% increase by 2026.

Of the suitable tailings materials, the highest annual tailings production comes from PGM layered mafic intrusions – estimated at ~2.1 Gt (mean value) in 2030 based on current commodity production and anticipated market growth (Fig. 1 and Supplementary Material B). This could lead to an accumulation of some 41 Gt total tailings by 2050 and 145 Gt by 2100 (mean values, assuming constant production from 2030 onwards). Ni sulphides and diamond kimberlites are anticipated to produce between 107 Mt (Ni sulphides) and 231 Mt (diamond kimberlites) tailings in 2030, while olivine dunites are expected to produce some 45 Mt in 2030. Serpentinite-hosted asbestos and talc deposits are expected to produce on average a combined ~6 Mt of tailings in 2030 (Fig. 1). In terms of CDR achievable annually, all suitable tailings show a rapid *a*CDR increase in the initial years of weathering, coinciding with the weathering period of both olivine and serpentine before both minerals are fully dissolved. The average *a*CDR across all suitable tailings is ~91 $MtCO_2$ (unimproved conditions) to ~458 $MtCO_2$ (improved conditions) across an operational period of 70 years (2030-2100), dominated by contributions from PGM layered mafic intrusions (averaging ~61 Mt CO_2 to 287 $MtCO_2$), primarily due to very large production rates. Other *a*CDR for tailings range, on average, from 0.03 $MtCO_2$ (asbestos serpentinites under unimproved conditions) up to 76 $MtCO_2$ (diamond kimberlites under improved conditions).

411 The compiled data suggests that there are at least 30 countries currently producing suitable
412 tailings who could host appropriate CDR schemes. In addition, approximately 30 Mt of the anticipated
413 global production in 2030 is located in other, unidentified, nations (Fig. 3 and Supplementary Fig. B).
414 Of the 2.4 Gt of suitable tailings expected to be produced in 2030, a large portion comes from South
415 Africa (~1.1 Gt), which hosts abundant PGM and diamond-bearing deposits across the Bushveld
416 Complex and Kaapvaal Craton regions respectively. These commodity-rich regions also extend to areas
417 of Botswana, Lesotho, and Zimbabwe, which may produce, together, around 194 Mt suitable tailings
418 in 2030. Other high producing countries include Russia, estimated to produce ~721 Mt of suitable
419 tailings in 2030, Canada (~222 Mt), and the United States (~102 Mt). See Supplementary Table E for
420 estimated national tailings production tonnages.

421 Values for *t*CDR and $\mathrm{E}_{pot}^{op,i}$ presented in Table 4 are based on average (mean) estimated tailings
422 production for the first year (2030-2031), the first 20 years (2030-2050) and a 70-year period (2030-
423 2100), for both unimproved and improved conditions. In terms of $\mathrm{E}_{pot}^{op,i}$, which shows, on average, how
424 much CDR can be achieved for every 1 kg of tailings fed into an implemented CDR operation for a given
425 period of time, olivine dunite (under improved conditions) shows the highest values (0.36, 0.84, and
426 0.89 gCO_2/kg for the periods 2030-2031, 2030-2050, and 2030-2100 respectively), followed by
427 asbestos serpentinites and PGM layered mafic intrusion tailings. Results also suggest that ~147 Mt
428 *t*CDR from 2030-2031 is achievable across all suitable mine tailings if materials are subjected to
429 improved EW conditions for the same time period (Table 4). By 2050, the total *t*CDR, with annual
430 tailings replenishment contributing to the overall total, for the suitable tailings is ~0.6-7.6 $GtCO_2$ (the
431 lower value achieved under unimproved conditions and upper value by improved conditions), and by
432 2100, ~6.5-32.5 $GtCO_2$, predominantly from voluminous PGM layered mafic intrusion tailings.
433 Approximately half of these totals comes from South African tailings, with Russia, and Canada also
434 having the capacity to make notable contributions primarily due to their PGM deposits.

Contributions towards global offset targets and counteracting national emissions have been calculated based on the mean *a*CDR of each suitable tailings material, averaged over a 70-year period of operation (Fig. 4). South Africa (~1.6%), Russia (~1.3%), Canada (~0.4%), and Zimbabwe (~0.23%) are the only countries that show a potential contribution of >0.2% towards global offset targets for unimproved conditions, reaching ~7.5% for South Africa, and ~6.2% for Russia under improved conditions. While their overall contribution to CDR on a global scale is modest under unimproved conditions, tailings-based CDR schemes in countries such as Botswana, Congo, Sierra Leone, Zimbabwe, and Norway could make significant contributions to offsetting their own CO_2 emissions (Fig. 4; Supplementary Table F), particularly under improved conditions. Botswana has particularly high offset potential, with the possibility of offsetting ~42% of emissions in tailings under unimproved reaction conditions (from a starting point of 2030), or even offsetting up to 219% of their national contributions (net negative) if any improved conditions could be utilised on all their produced suitable tailings (Fig. 4; Supplementary Table F). Congo could reach up to ~92% offset potential under improved conditions, while Zimbabwe shows an offset potential of ~11-54%.

4. Discussion

4.1. Material considerations and suitable host nations

Based on the criteria applied in this study, the list of the most suitable mine tailings for CDR purposes are those associated with the following commodities and host rocks:

- Asbestos and talc serpentinite deposits
- Diamond kimberlites
- Ni sulphide deposits
- Olivine dunites
- PGM layered mafic intrusions

Though these six tailings material types may not be universally suitable, they generally contain favourable mineral types and modal abundances. This suitability is based on their calculated *s*CDR values, which essentially provide a new E_{pot} value that reflects both mineral kinetics and reaction timescales, with the values changing over time based on shrinking core modelling. Tailings associated with Cu porphyry and VMS, Ti anorthosite, Cr layered and podiform deposits, and Pb-Zn skarn deposits may also be partially suitable, but based on their slow kinetics and overall low CDR volumes on decadal timescales, they would generally need to be considered on an individual site-by-site basis. As this assessment is based purely on the targetable silicate mineral content, it does not consider the presence of minor non-silicate phases such as the kinetically favourable (in terms of both W_r and E_{pot}) brucite, which could make a significant difference to the CDR (Harrison et al., 2013, 2015; Zarandi et al., 2021). Tailings such as those associated with Ni sulphides, kimberlites, and serpentinites are known to contain variable amounts of brucite, which could improve the kinetic ranking and overall CDR capacity of a given deposit. Offering high production tonnages, PGM layered mafic intrusions dominate the both the average and overall (sum) contributions to *a*CDR across all suitable tailings, warranting a greater focus in future CDR studies.

The estimate of annual CDR potential through weathering of all mine tailings made by Bullock et al. (2021) on the basis of chemical favourability, was 1.1 to 4.5 Gt CO_2/year, with a mean estimate of 2.4 Gt CO_2/year. In this study, where in addition mineral kinetics are considered, the average annual CDR potential (averaged over a 70-year period) is found to vary from about 93 (unimproved conditions) to 465 (improved conditions) Mt/year. This difference is also reflected in the difference between the original whole rock E_{pot} values (Bullock et al., 2021) and the newly calculated CDR capacities and $\mathrm{E}_{pot}^{op,i}$ derived for a given period of operation. For example, we note an E_{pot} range, based on chemical favourability only, from 558 (diamond kimberlite) to 722 gCO_2/kg (talc serpentinite), while the averaged *s*CDR range (over 70 years) is ~34 (asbestos serpentinite) to 197 gCO_2/kg (olivine dunite) for unimproved reaction conditions, or ~330 (diamond kimberlite) to 873 gCO_2/kg (olivine dunite) for improved conditions.

The difference between the hypothetical maximum CDR capacity based on material chemistry and the kinetically-informed CDR capacity under unimproved conditions underlines the importance of mineral kinetics, and the need to speed up reactions to unlock the high chemical potential of many waste minerals found in tailings, particularly pyroxenes and feldspars. The difference also suggests the necessity to make efforts to utilise other tailings materials of variable potential, such as Cu, Ti, Cr, and Pb-Zn deposits, which could form a significant resource for CDR. Indeed, much of the overall CDR of Bullock et al. (2021) is attributed to Cu deposits, but the lack of kinetic favourability identified here means that these deposits cannot yet be considered suitable for CDR purposes.

There are several important caveats to this material kinetic assessment. The modal mineralogies of the different materials were selected from published studies without bias and based on their data availability, and applied to a given tailings type without modal variation. It should be stressed that available published W_r data for the targetable minerals can be both wide ranging (e.g., plagioclase W_r values) for a given set of constrained experimental parameters, resulting in associated uncertainty in the selection and usage of the data, or in some instances, limited to few studies or data points. This underlines the importance of more studies focused on constraining dissolution rates of minerals and rocks, including mine tailings. There is also inherent variability in tailings modal mineralogies. Mineral contents of the host rocks can vary across regions and even within mine sites, so deposits can show both high and low CDR potential, directly related to the mineralogy of a given material. The variations in mineral end members are also important, as plagioclase minerals show a wide range of W_r values based on their variable chemistry (Supplementary Table B). In terms of grain size, tailings can show a wide and variable grain size distribution, with some finer minerals that are present likely to dissolve faster than coarser minerals. Some materials may also be, on average, coarser or finer than the example values presented here for a given operation (see Supplementary Material A), which will affect the kinetics and rates of CDR (see below). If an operation that produces coarse grained (>100 μm) tailings has the capability to grind materials to finer (<100 μm) grain sizes, this could further improve CDR at particular mine sites.

511

512 **4.2. The role of enhanced weathering**

513 The "unimproved" kinetic parameters reported here were generally selected from experiments and
514 simulations at near-neutral pH and ambient pCO_2 and temperature conditions. The ability, in
515 appropriately engineered schemes to shift conditions to slightly, or even highly acidic or alkaline
516 conditions, or to apply additional EW methods such as elevated pCO_2 and temperature, could greatly
517 increase rates of CDR. Under the applied improved conditions of this study, olivine, and serpentine
518 show very fast reaction kinetics, achieving full dissolution in 3-8 years (Supplementary Table D).
519 Clinopyroxene may also effectively undergo full dissolution in 70 years, while plagioclase may take up
520 to ~315 years (Supplementary Table D). These improved conditions may be more easily achievable for
521 certain mine sites, perhaps benefiting from more favourable climates (e.g., hot conditions all year
522 round), or having proximal access to a CO_2 point source (e.g., CO_2-rich flue gases) to increase pCO_2.
523 The effect of the improved conditions applied in this study to tailings is an increase in $E_{pot}^{op,i}$, *t*CDR,
524 *s*CDR and *a*CDR across all materials compared to the same calculations under unimproved conditions
525 (Tables 2 and 4, and Figs. 1-4). This includes notable increases to *s*CDR associated with Cu porphyry
526 and VMS, Cr layered intrusives, Ti anorthosite, and Pb-Zn skarn deposits, though their overall *s*CDR is
527 still generally less than 100 g per 1 kg of material over 70 years.

528 While improvement through grain size reduction to 10 µm, utilised here as a lower limit size,
529 or generating solution conditions of pH 3-4, may be achievable, some operators may not have the
530 capabilities to implement these steps. For instance, a particle size as fine as 10 µm may lead to
531 difficulties in batch reaction processes and any required storage management. However, in practice,
532 mine operators are more likely to be able to achieve finer grain sizes as opposed to maintaining an
533 acidic solution environment, as crushing and grinding are a conventional part of the concentration
534 process. Applying the shrinking core model here to typical minerals such as olivine, clinopyroxene,
535 orthopyroxene, biotite, and serpentine show that the choice of intervention to increase weathering

rate depends on the deposit type. For example, for olivine and serpentine, a grain size of 100 µm and acidic pH has a greater CDR than 10 µm and neutral pH. Conversely, for orthopyroxene, clinopyroxene, and biotite, a reduction to 10 µm and neutral pH solution has a higher CDR than at 100 µm and pH 3-4 acidic solution. Tailings that contain higher amounts of the orthopyroxene, clinopyroxene, and biotite, such as PGM layered mafic intrusion tailings, could benefit more from grinding smaller than from a pH reduction. Conversely, weathering of olivine- and serpentine-rich tailings (e.g., kimberlites, serpentinites, Ni sulphides) might be accelerated by acidic conditions in a reactor or contained pond setting.

Based on the shrinking core modelling of this study, the rate of CDR lessens drastically once the fastest reacting minerals (olivine, serpentine, clinopyroxene, and, in some instances, plagioclase) have undergone full dissolution. This may mean that the optimal approach is to focus on the dissolution of these fast-reacting minerals (e.g., the olivine, serpentine, clinopyroxene, and plagioclase) on relatively short timescales, and to treat the remaining minerals as typical waste minerals. The slow reaction kinetics of minerals such as orthopyroxene, amphibole, and biotite mean that CDR will occur, but the amounts of removal will be limited. One approach could be to separate the olivine, serpentine, clinopyroxene, and plagioclase for CDR-focused reactions. Alternatively, one could simply start with reacting all targetable minerals but terminate the operation after the fast-reacting minerals have been converted and move and store the remaining minerals, as further processing the remaining minerals might not justify the spatial, energy and financial costs.

Suggestions for improved reaction conditions need to be feasible for a given mine operation, considering the implications for additional costs, energy inputs, greenhouse gas emissions, and other environmental impacts, which might result from changes to operating temperature or acidity of solutions (e.g., pH <2). However, acidic conditions of pH 3-4 may still be highly beneficial for EW, and could perhaps be attained using microbial additions, through use of chemical additives, and/or by supplying a higher pCO_2 in any utilised reactor system (e.g., by the addition of direct air capture (DAC)

561 or flue gases). There may, for instance, be on-site opportunities to take advantage of microbiological
562 acceleration, whereby microbial metabolisms are exploited to achieve EW (e.g., Salek et al., 2013,
563 Power et al., 2014).

564

565 **4.3. Alkalinity generation vs. carbonate precipitation**

566 An important consideration for implementation of any CDR method on a mine site is the fate of the
567 reaction product, which may be alkalinity (captured CO_2 as bicarbonate in water) and/or solid
568 carbonate minerals. As previously discussed, alkalinity production is the favoured route for CDR, as
569 more CO_2 is removed by this approach. There are inherent spatial advantages to CDR by alkalinity
570 production, as an additional precipitation step may require some method of initiating carbonation.
571 There is also the consideration that introducing additional alkalinity to the ocean could mitigate the
572 effects of ocean acidification caused by uptake of anthropogenic CO_2 (Hartmann et al., 2013; Renforth
573 and Henderson, 2017; Beerling et al., 2020). However, the effects of such concentrated alkalinity on
574 local river systems, groundwater systems, and coast-proximal ocean regions are not yet fully
575 understood, and the consequences of releasing large additional volumes of liquid effluent into these
576 systems (particularly for mines far from coastal regions) require more research. Generating alkalinity
577 requires a great deal of water input, with no option to reuse or recycle the bicarbonate-laden product
578 following CO_2-tailings reactions. It is therefore possible that, despite the lower CDR capacity,
579 precipitation of solid carbonates would be the desired means of final product storage for some mine
580 sites, such as those, and there are many, with constrained water supply. This would permit mines to
581 continue to store the materials on-site in new or existing tailings dams, as is standard practice for the
582 industry, and the process waters can be recycled. It should also be considered that by-product
583 recovery of pure SiO_2 and carbonates may provide both a secondary usage or revenue stream (e.g.,
584 use in aggregates, cements, or backfill). Storage of carbonate minerals also does not require post-

storage environmental monitoring (Lackner et al., 1995; Sipilä et al., 2008; Power et al., 2013; Boot-Handford et al., 2014).

Precipitation of carbonates is, in general, not considered a rate-limiting step in the entire carbonation process (i.e., silicate mineral dissolution, CO_2 dissolution, and hydration, secondary carbonate mineral formation) by studies focused on ultramafic mine tailings (e.g., Wilson et al., 2010; Harrison et al., 2013; Power et al., 2013; Li et al., 2018; Wang et al., 2020). Akin to hydration rate, carbonation rate has been suggested to associate well with dissolution rate properties of minerals that control the diffusion rate of Ca^{2+} in a CO_2-containing solution (Wang et al., 2020). High degrees of supersaturation have been shown to correspond with highest rates of carbonation, due to the development of the most nucleation sites in a reaction (Wang et al., 2020). This assumption is further supported by evidence of secondary carbonate precipitation at several mine sites or in association with mine tailings, without deliberate attempts to initiate carbonation (i.e., 'passive' carbonation). For instance, hydromagnesite has been shown to precipitate at the Woodsreef asbestos mine (Oskierski et al., 2013) and Mount Keith nickel mine (Wilson et al., 2014) in Australia, while similar observations were also made at the Diavik diamond mine and Clinton Creek asbestos mine, Canada (Power et al., 2013). The formation of more stable but kinetically inhibited Mg-carbonates may require additional conditions, such as increasing temperature, pH, presence of ligands, and microbial mediation (O'Neil and Barnes, 1971; Giammar et al., 2005; Morse et al., 2007; Power et al., 2013, 2014, 2016; Hänchen et al., 2008; Saldi et al., 2009, 2010, 2012; Schott et al., 2009; Wilson et al., 2009a, 2010; Case et al. 2011; Haug et al. 2011; Power et al., 2013; Li et al., 2018; Wang et al., 2020).

It is critical to achieve a balance between accelerated silicate dissolution and subsequent carbonate precipitation, without compromising one or both processes. This may require two or more separate stages of complete carbonation, where a single reactor system (or other means of achieving the desired reactions) is not sufficient for both accelerated dissolution and precipitation steps. The challenge is to determine the most appropriate method for a given site and material, such as chemical

610 reactor approaches (Xing et al., 2021), through heap leaching (Li et al., 2018), air sparging (Power et
611 al., 2014; Wilson et al., 2014) or injections into new or existing tailings dams (Power et al., 2020). For
612 utilising heat, local heat producing smelter operations, or any heat "waste" produced during
613 extraction or concentration, could be harnessed and used as an additional EW method to speed up
614 batch reactions. This may also be the case for utilising high pCO_2 on site (where evident), or by
615 harnessing any CO_2-rich gases from nearby sites via gas pipelines. Site-proximal flue gas supplies, such
616 as those sourced from cement producing operations and electricity-generating power stations, may
617 provide an effective source of CO_2 for accelerated carbonation rates (e.g., Matter et al., 2011, 2016;
618 Pu et al., 2021), possibly helping to overcome practical limitations and supply issues associated with
619 the use of pure CO_2. For example, carbonation extent through use of flue gases with <20% CO_2 have
620 been shown to be comparable to commercially mixed gases containing CO_2 >20% (Pu et al., 2021).
621 Alternatively, incorporation of a hybrid EW-DAC system may be an option that warrants further
622 investigation, as well as field and/or off-site methods such as similar rock EW-based field and coastal
623 spreading approaches (Schuiling and Krijgsman, 2006; ten Berge et al., 2012), and incorporation into
624 agricultural soils (Corti et al., 2012; Edwards et al., 2017; Andrews and Taylor, 2019; Beerling et al.,
625 2020; James et al., 2021).

626

627 **4.4. Global and national assessment**

628 The nation-by-nation assessment suggests that South Africa, Russia, Canada, Zimbabwe, and the
629 United States hold the highest capacity for CDR (and therefore globally-relevant CDR contributions)
630 through alkalinity generation (Fig. 4; Supplementary Table F) and/or carbonation of mine tailings.
631 These countries may therefore benefit from future CDR investigations and large-scale pilot schemes.
632 Several African nations, including Botswana, Congo, Sierra Leone, Lesotho, and Angola, also show a
633 high potential to offset their own CO_2 emissions through this route (Fig. 4; Supplementary Table F),
634 particularly when tailings are subjected to improved conditions. There is an additional incentive to

635 pursue a route that incorporates EW into any applied CDR scheme in countries such as Angola, Brazil,
636 Congo, Guinea, India, Mexico, Sierra Leone, and Tanzania, as EW could be more effective in tropical
637 climates where higher temperatures and/or rainfall promote higher chemical weathering rates
638 (Supplementary Fig. D; Edwards et al. 2017; Andrews and Taylor, 2019).

639 Estimated overall contributions of suitable tailings CO_2 removal targets are uneven by
640 individual countries (Fig. 4c-d and Supplementary Table F) but combined globally could make a notable
641 impact. Taking a lower global removal target of 2 Gt per year (projections of rapid technological
642 change could require a lower requirement of 2-2.5 Gt CO_2 extraction goals; Mercure et al., 2018;
643 Beerling et al., 2020), alkalinity production of suitable mine tailings has the potential to contribute a
644 global total of ~4% (under unimproved reaction conditions) up to ~23% (under improved conditions).
645 These values may not fully reflect the overall possible contribution to CDR through alkalinity
646 generation of suitable mine tailings. The CDR values presented here are based on average (mean)
647 estimated tailings production, but if maximum values are realised, or market growth and production
648 exceed the estimates made in this study, more tailings material could be available leading to higher
649 rates of CDR. For instance, maximum tailings estimates made here are ~6.6 Gt in 2030, almost three
650 times the mean estimate. Also, if some or all of the tailings associated with Cu porphyry and VMS, Cr
651 layered and podiform, Pb-Zn skarn, and Ti anorthosite materials can be effectively utilised for CDR
652 purposes, this would give on average an additional ~17 Gt of tailings material by 2030, which would
653 provide a vast extra amount of material for CDR. If tailings associated with Cr, Cu, Pb-Zn, and Ti could
654 be better utilised through improved means of EW, the maximum CDR potential will also increase,
655 involving additional host countries such as Bolivia, Chile, Madagascar, Mongolia, Peru, Philippines,
656 Poland, Sweden, and Zambia (indicated by grey colour in Figs. 3-4).

657 Estimates made here do not account for any future increases in commodity demand and
658 market growth (and therefore tailings production and CDR capacity) over the period 2030-2100, which
659 could increase the CDR capacity of mine tailings. Additionally, if historic tailings were targeted, there

660 might be potential for some really large CDR schemes. Some historic tailings dams at active sites have
661 accumulated material for 50 to >100 years. For example, the Cullinan diamond mine in South Africa
662 has been operating since 1903 (Cornish, 2013). Other examples include the Sudbury nickel mines,
663 operating since 1920 (Mining Association of Canada, 2014), Kristineberg polymetallic mine in Sweden,
664 operating since 1940 (Heikkinen et al., 2008), and Rustenburg platinum operations in South Africa,
665 active since the 1970s (Jubileus, 2008). Though difficult to quantify, these historic tailings, coupled
666 with utilisation of inactive and abandoned operations for CDR purposes, could offer a scale of suitable
667 material capable of significantly contributing to CDR targets.

668 The calculations and assessments reported here draw attention to the urgent need for more
669 research in this area. For example, dissolution rates taken from literature for individual minerals were
670 measured under specific experimental conditions, unique to each particular study. Some data is
671 therefore limited in scope, probably not truly reflective of these heterogeneous materials. The mineral
672 composition of tailings can vary from sample to sample, reflecting variations in the host rock geology,
673 which can also vary across a site. Minerals themselves can vary in geochemistry between host rocks
674 and across geographic regions. Much more research on different tailings types is required to provide
675 the geochemical and mineralogical data needed to calculate the global CDR potential of these valuable
676 resources. Grain size can vary widely between sites, with size distributions, rather than a single,
677 uniform size, typical for a given operation - again, very many more individual site or location studies
678 are needed with reporting of detailed mineral and rock characterisation and CO_2 reactivity
679 experimentation. In terms of estimated tailings production rates from 2030 to 2100, these are
680 assumed here to be constant. In reality, rates will fluctuate based on commodity demand, changes to
681 production efficiency and efforts to reduce waste production or excessive mining activities at sites;
682 more work is required on future trends in tailings production, particularly of the key mineral types
683 identified here as promising for CDR. Implementation of practical acceleration techniques related to
684 the existing biology, geology, and hydrology will require detailed engineering, environmental,
685 legislative, and economic considerations for targetable sites and regions, such as those in Southern

686 Africa, Russia, and North America. A practical consideration that needs to be researched is the
687 potential liberation of environmentally damaging trace elements, such as Ni and Cr. It is beyond the
688 scope of this study to provide a detailed assessment and possible solutions to trace element-laden
689 water outputs that may arise from any implemented CDR scheme, but it is important to examine this
690 issue. Mine sites are well equipped for identifying, monitoring, maintaining, and resolving
691 environmental impacts associated with their activities, so any weathering scheme should be able to
692 form part of the conventional management system that is already in place. Theoretical capacity
693 calculations, lab-scale experiments, practical assessments, pilot studies, and field trials are the first
694 steps to address these factors and to realise the high site potential for CDR on a scale of millions of
695 tonnes for host countries and promising regions detailed in this study.

696

697 **5. Conclusions**

698 The role of mineral weathering kinetics is a vital consideration in the overall assessment the suitability
699 of mine tailings to bring about CDR. While some minerals host the right chemical composition for
700 reactions with CO_2 to produce bicarbonate alkalinity and carbonate solids, dissolution rates are often
701 too slow to achieve significant CDR on timescales relevant for climate change mitigation. In this study,
702 31 silicate-hosted mine tailings were assessed for suitability for CDR by alkalinity production and
703 mineral carbonation. According to their overall capacity for CDR based on their whole rock
704 composition and contained mineral chemistry, their global production volumes, and the favourability
705 of the reaction kinetics expected of their mineral content, six of these tailings types were deemed to
706 be highly suitable for targeted CDR mine site implementation:

707 • Asbestos and talc serpentinite deposits
708 • Diamond kimberlites
709 • Ni sulphide deposits
710 • Olivine dunites

- PGM layered mafic intrusions, the dominating contribution due to high production tonnages

Other materials, such as those produced from Cr layered and podiform deposits, Cu porphyry and VMS deposits, Ti anorthosites, and Pb-Zn skarn deposits, may also be suitable, though their variable mineral contents means that their possible usage for CDR requires further consideration. The most suitable deposits show variable potential for offsetting national CO_2 outputs and to the global movement to remove CO_2 for globally relevant CDR targets and timescales. This potential can be increased by methods to improve the weathering rate, such as reactions in lower pH solutions and grinding to smaller particle size. Mining operations of South Africa, Canada, and Russia could make significant contributions to global CDR targets, and several African countries could potentially offset their own CO_2 emissions through EW of suitable tailings. For EW of tailings, tropical countries have the natural advantage of higher ambient temperatures and greater rainfall which could help provide additional EW conditions, if material processing and storage measures can be suitably adapted. By 2100, the total cumulative CDR, with annual tailings replenishment contributing to the overall total, for all suitable tailings could reach ~32.5 $GtCO_2$ if reaction conditions are enhanced, predominantly due to high production volumes of PGM layered mafic intrusion tailings. High-producing countries could potentially contribute up to ~7.5% towards global emission reduction targets, or offset some or all of their own CO_2 emissions outputs. The large inventory of many historic tailings, in dams and stockpiles, also offers the potential for significant contribution to emission offsets and global CDR targets.

The next steps for large-scale CDR implementation are to make further assessments of the practicalities of incorporating such EW methods into the processing systems of active (and possibly inactive or abandoned) mine sites. Further research is needed to establish effective and practical methods for CDR by EW (e.g., reactor systems, EW implementation in new or existing tailings dams, or field and off-site opportunities). The recognition of spatial and resource requirements, and appropriate management of products and by-products need more attention. More research is also

urgently needed on the properties of suitable mineral and tailings inventories, particularly the measurement of weathering kinetics under a variety of potential reaction conditions.

Table captions

Table 1. List of selected silicate-hosted mine tailings (classified by their targeted commodity and typical host rock) for initial assessment of CDR potential (after Bullock et al., 2021).

Table 2. Typical targetable minerals (selected based on their favourable Ca-Mg content and mineral E_{pot}) found in the assessed tailings deposits, and their kinetic properties. Dissolution rates (W_r) include published rates achieved under "unimproved" (near-neutral) conditions ("Neut" - mean values of published experimental W_r achieved at solution pH 6-8, temperature 21-24°C, ambient pCO_2) or under any applied reaction conditions ("any").

Table 3. Estimates of dissolution extent over time (on decadal timescales of up to 70 years) for a theoretical 1 kg of tailings material at typical grain sizes (Table 1) and unimproved conditions (using W_r^{Neut}; see Tables 1-2 and Supplementary Material B). Assessment undertaken to aid determination of most suitable tailings materials for CDR purposes for tailings deemed potentially chemically favourable (see text). Calculated *s*CDR potential over 70 years also shown as gCO_2 removed as alkalinity. Maximum and minimum values shown in brackets to account for variations in W_r^{Neut} (Tables 1-2). Minerals present and estimated modal content of tailings based on information presented in Table 3, with unwanted minerals (e.g., sulphides, Fe oxides) not listed (though their weighted contribution to theoretical 1 kg of material has been factored in to calculations).

Table 4. Total cumulative CDR (*t*CDR; $MtCO_2$ as alkalinity) based on annual tailings production estimates, and average $E_{pot}^{op,i}$ of 1 kg of suitable tailings (CO_2 removed as alkalinity) after 1-70 years of operation, both under unimproved and improved reaction conditions (from implementation in 2030 onwards). Calculated values are based on mean annual and mean cumulative production estimates from Table 3.

Figure captions

Fig. 1. Boxcharts showing estimated production rate of suitable mine tailings for CDR purposes for 2030 (based on 2020 production and anticipated market growth), with 2050 and 2100 tonnages showing amount accumulated each year at constant production rates from 2030.

Fig. 2. Calculated average *s*CDR for 1 kg of material (averaged over period 2030-2100) versus estimated average annual tailings production for the most suitable tailings based on selection criteria in this study, presented for alkalinity generation under both unimproved and improved conditions for all suitable tailings. Error bars represent estimated range in production (X axis) and total range of *s*CDR values from 2030 up to 2100 (Y axis) [COLOUR PRINT; 2-COLUMN]

Fig. 3. CDR achieved annually (*a*CDR) for each suitable tailings material, and the total *a*CDR for all suitable tailings, shown under unimproved (U) and improved conditions (I). [COLOUR PRINT; 2-COLUMN]

Fig. 4. Countries identified as hosting suitable mine tailings of variable CDR potential, with their average *a*CDR (presented as Mt/year of CO_2 removed through alkalinity generation) between 2030-2100 shown for (a) unimproved reaction conditions, and (b) considering the implementation of improved conditions on grain size and reaction solution pH. Countries that may show some minor CDR potential but are currently limited due to slow reaction kinetics of their host minerals, are highlighted in grey. [COLOUR PRINT; 2-COLUMN]

Fig. 5. Potential offset contributions (% of emissions or targeted removal tonnages) that could be theoretically made by annual CDR (quantified by average *a*CDR between 2030 and 2070) through alkalinity generation of mine tailings in suitable host countries: (a) contributions to national CO_2 emissions under unimproved reaction conditions, (b) contributions to offsetting emissions under improved conditions, (c) contributions to a global CDR target (2 Gt/year) under unimproved reaction conditions, and (d) contributions to a global CDR target (2 Gt/year) under improved conditions. [COLOUR PRINT; 2-COLUMN; 2 PAGES]

Competing interests: The authors have no competing interests to declare.

Author Contributions: The manuscript was written through contributions of all authors. All authors have given approval to the final version of the manuscript.

Funding: The GGREW project (NE/P019536/1) is supported by NERC, the Engineering & Physical Sciences Research Council (EPSRC), the Economic & Social Research Council (ESRC), and the Department for Business, Energy & Industrial Strategy (BEIS), with in-kind contributions from the Met Office Hadley Centre and the Science & Technology Facilities Council (STFC).

References

Andrews, M. G., and Taylor, L. L. (2019). Combating climate change through enhanced weathering of agricultural soils. Elements 15, 253-258. doi: 10.2138/gselements.15.4.253

Assima, G.P., Larachi, F., Molson, J., and Beaudoin, G. (2014). Emulation of ambient carbon dioxide diffusion and carbonation within nickel mining residues. Miner. Eng. 59, 39-44. doi: 10.1016/j.mineng.2013.09.002

Bandstra, J. Z., Buss, H. L., Campen, R. K., Liermann, L. J., Moore, J., Hausrath, E. M., et al. (2008). "Appendix: Compilation of mineral dissolution rates," in Kinetics of Water-Rock Interaction, eds. S. L. Brantley, J. D. Kubicki and A. F. White (New York: Springer), 737-823.

Beerling, D. J., Kantzas, E. P., Lomas, M. R., Wade, P., Eufrasio, R. M., Renforth, P., et al. (2020). Potential for large-scale CO_2 removal via enhanced rock weathering with croplands. Nature 583, 242-248. doi: 10.1038/s41586-020-2448-9

Bodénan, F., Bourgeois, F., Petiot, C., Aug,é, T., Bonfils, B., Julcour-Lebigue, C., et al. (2014). Ex situ mineral carbonation for CO_2 mitigation: Evaluation of mining waste resources, aqueous carbonation processability and life cycle assessment (Carmex project). Miner. Eng. 59, 52-63. doi: 10.1016/j.mineng.2014.01.011

Boot-Handford, M.E., Abanades, J.C., Anthony, E.J., Blunt, M.J., Brandani, S., MacDowell, N., et al., (2014). Carbon capture and storage update. Energy Environ. Sci. 7, 130-189. doi: 10.1039/C3EE42350F

Bullock, L.A., James, R.H., Matter, J., Renforth, P., and Teagle, D.A.H. (2021) Global carbon dioxide removal potential of waste materials from metal and diamond mining, Front. Clim. 3, 694175. doi: 10.3389/fclim.2021.694175

Canadell, J. G., Le Quéré, C., Raupach, M. R., Field, C. B., Buitenhuis, E. T., Ciais, P., et al. (2007). Contributions to accelerating atmospheric CO_2 growth from economic activity, carbon intensity, and efficiency of natural sinks. Proc. Natl. Acad. Sci. U.S.A. 104, 18866-18870. doi: 10.1073/pnas.0702737104

Cornish, L., (2013). Cullinan reveals its true colours. Inside Mining 6, 1, 28-32.

Corti, G., Weindorf, D. C., Fernandez Sanjurjo, M. J., and Cacovean, H. (2012). Use of waste materials to452 improve soil fertility and increase crop quality and quantity. Appl. Environ. Soil Sci. 2012:204914 doi: 10.1155/2012/204914

Darton, R. C., and Yang, A. (2020). "Removing carbon dioxide from the air to stabilise the climate," in Advances in Carbon Management Technologies, eds. S. K. Sidkar and F. Priciotta (Boca Raton: CRC Press), 3-22.

Dichicco, M.C., Paternoster, M., Rizzo, G., and Sinisi, R., (2015). Mineralogical asbestos assessment in the Southern Apennines (Italy): A review. Fibres 7, 24. doi: 10.3390/fib7030024

Dudhaiya, A., Haque, F., Fantucci, H., and Santos, R. M. (2019). Characterization of physically fractionated wollastonite-amended agricultural soils. Minerals 9:635. doi: 10.3390/min9100635

Dunn, F., and Vietti, A., (2003). The thirsty business of diamond mining, 4th One Day Seminar on Hydraulic Transport in the Mining Industry, Hydraulic Conveying Association of South Africa, Johannesburg (HCASA), April 7, Paper A.

Edwards, D. P., Lim, F., James, R. H., Pearce, C. R., Scholes, J., Freckleton, R. P., et al. (2017). Climate change mitigation: potential benefits and pitfalls of enhanced rock weathering in tropical agriculture. Biol. Lett. 13:20160715. doi: 10.1098/rsbl.2016.0715

Field, C. B., and Raupach, M. R. (2004). The Global Carbon Cycle: Integrating humans, climate and the natural world. Washington, DC: Island Press.

Giammar, D.E., Bruant, R.G., and Peters, C.A., (2005). Forsterite dissolution and magnesite precipitation at conditions relevant for deep saline aquifer storage and sequestration of carbon dioxide Chem. Geol., 217, 257-276. doi: 10.1016/j.chemgeo.2004.12.013

834 Hänchen, M., Prigiobbe, V., Baciocchi, R., and Mazzotti, M. (2008) Precipitation in the Mg-carbonate system -
835 effects of temperature and CO_2 pressure. Chem. Eng. Sci., 63, 1012−1028. doi: 10.1016/j.ces.2007.09.052

836 Hänchen, M., Prigiobbe, V., Storti, G., Seward, T.M., and Mazzotti, M., (2006). Dissolution kinetics of fosteritic
837 olivine at 90–150 °C including effects of the presence of CO_2. Geochim. Cosmochim. Acta 70, 4403-4416. doi:
838 10.1016/j.gca.2006.06.1560

839 Hangx, S. J. T., and Spiers, C. J. (2009). Coastal spreading of olivine to control atmospheric CO_2 concentrations: a
840 critical analysis of viability. Int. J. Greenhouse Gas Control 3, 757-767. doi: 10.1016/j.ijggc.2009.07.001

841 Haque, F., Santos, R. M., Dutta, A., Thimmanagari, M., and Chiang, Y. W. (2019). Co-benefits of wollastonite
842 weathering in agriculture: CO_2 sequestration and promoted plant growth. ACS Omega 4, 1425-1433. doi:
843 10.1021/acsomega.8b02477

844 Harrison, A. L., Power, I. M., and Dipple, G. M. (2013). Accelerated carbonation of brucite in mine tailings for
845 carbon sequestration. Environ. Sci. Technol. 47, 126-134. doi: 10.1021/es3012854

846 Harrison, A.L., Dipple, G.M., Power, I.M., and Ulrich Mayer, K., (2015). Influence of surface passivation and water
847 content on mineral reactions in unsaturated porous media: implications for brucite carbonation and CO_2
848 sequestration. Geochim. Cosmochim. Acta 148, 477–495. doi: 10.1016/j.gca.2014.10.020

849 Hartmann, J., West, A. J., Renforth, P., Köhler, P., De La Rocha, C. L., Wolf-Gladrow, D. A., et al. (2013). Enhanced
850 chemical weathering as a geoengineering strategy to reduce atmospheric carbon dioxide, supply nutrients, and
851 mitigate ocean acidification. Rev. Geophys. 51, 113-149. doi: 10.1002/rog.20004

852 Heikkinen, P.M., Noras, P., Salminen, R., Mroueh, U.-M., Vahanne, P., Wahlström, M.M., et al., (2008).
853 Environmental techniques for the extractive industries. Mine Closure Handbook, Espoo, 2008.

854 Hietkamp, S., Engelbrecht, A., Scholes, B., and Golding, A. (2004). Carbon capture and storage in South Africa.
855 CSIR, 1–7.

856 Hitch, M., Ballantyne, S. M., and Hindle, S. R. (2010). Revaluing mine waste rock for carbon capture and storage.
857 Int. J. Min. Reclamat. Environ. 24, 64-79. doi: 10.1080/17480930902843102

IPCC (Intergovernmental Panel on Climate Change) (2018). Climate Change 2013: Global Warming of 1.5°C. Geneva: IPCC.

IPCC (Intergovernmental Panel on Climate Change) (2019). IPCC Special Report on the Ocean and Cryosphere in a Changing Climate. Geneva: IPCC.

James, R.H., Bullock. L.A., Larkin, C., and Matter, J., (2021). Geological solutions for carbon dioxide removal. Geoscientist Magazine, Autumn Edition, 16-22.

Jubileus, M.T., (2008). Assessment of platinum mine tailings storage facilities: An ecotoxicological perspective. MSc. Thesis, North-West University, South Africa.

Kelemen, P. B., McQueen, N.,Wilcox, J., Renforth, P., Dipple, G., and Vankeuren, A. P. (2020). Engineered carbon mineralization in ultramafic rocks for CO_2 removal from air: review and new insights. Chem. Geol. 550:119628. doi: 10.1016/j.chemgeo.2020.119628

Kelemen, P., Benson, S.M., Pilorgé, H., Psarras, P., and Wilcox, J. (2019). An overview of the status and challenges of CO_2 storage in minerals and geological formations. Front. Clim. 1, 9. doi: 10.3389/fclim.2019.00009

Kesler, S. E., and Simon, A. C. (2015). Mineral Resources, Economics and the Environment, 2nd Edition. Cambridge: Cambridge University Press.

Kremer, D., Etzold, S., Boldt, J., Blaum, P., Hahn, K.M.,Wotruba, H., et al. (2019). Geological mapping and characterization of possible primary input materials for the mineral sequestration of carbon dioxide in Europe. Minerals 9:485. doi: 10.3390/min9080485

Krevor, S., and Lackner, K.S., (2011). Enhancing serpentine dissolution kinetics for mineral carbon dioxide sequestration. Int. J. Greenhouse Gas Control 5, 1073-1080. doi: 10.1016/j.ijggc.2011.01.006

Krevor, S.C., Graves, C.R., Van Gosen, B.S., and McCafferty, A., (2009). Mapping the mineral resource base for mineral carbon-dioxide sequestration in the conterminous United States. U.S. Geological Survey Digital Data Series 414.

881 Lacinska, A.M., Styles, M.T., Bateman, K., Hall, M., and Brown, P.D. (2017). An experimental study of the
882 carbonation of serpentinite and partially serpentinised peridotites. Front. Earth Sci. 5, 37. doi:
883 10.3389/feart.2017.00037

884 Lackner, K. S., Wendt, C. H., Butt, D. P., Joyce, E. L., and Sharp, D. H. (1995). Carbon dioxide disposal in carbonate
885 minerals. Energy 20, 1153-1170. doi: 10.1016/0360-5442(95)00071-N

886 Li, J., Hitch, M., Power, I. M., and Pan, Y. (2018). Integrated mineral carbonation of ultramafic mine deposits—a
887 review. Minerals 8:147. doi: 10.3390/min8040147

888 Matter, J., Broecker, W.S., Gislason, S.R., Gunnlaugsson, E., Oelkers, E.H., Stute, M., et al., (2011). The CarbFix
889 pilot project – Storing carbon dioxide in basalt. Energy Procedia 4, 5579–5585. doi:
890 10.1016/j.egypro.2011.02.546

891 Matter, J., Stute, M., Snæbjörnsdottir, S.Ó., Oelkers, E.H., Gislason, S.R., Aradottir, E.S., et al., (2016). Rapid
892 carbon mineralization for permanent disposal of anthropogenic carbon dioxide emissions. Science 352, 6291,
893 1312-1314. doi: 10.1126/science.aad8132

894 McCutcheon, J., Turvey, C., Wilson, S. A., Hamilton, J. L., and Southam, G. (2017). Experimental deployment of
895 microbial mineral carbonation at an asbestos mine: potential applications to carbon storage and tailings
896 stabilization. Minerals 7:191. doi: 10.3390/min7100191

897 McCutcheon, J., Wilson, S. A., and Southam, G. (2016). Microbially accelerated carbonate mineral precipitation
898 as a strategy for in situ carbon sequestration and rehabilitation of asbestos mine sites. Environ. Sci. Technol. 50,
899 1419-1427. doi: 10.1021/acs.est.5b04293

900 Mercure, J.-F., Pollitt, H., Viñuales, J.E., Edwards, N.R., Holden, P.B., Chewpreecha, U., et al., (2018).
901 Macroeconomic impact of stranded fossil fuel assets. Nat. Clim. Change 8, 588-593. doi: 10.1038/s41558-018-
902 0182-1

903 Mervine, E. M., Wilson, S. A., Power, I. M., Dipple, G. M., Turvey, C. C., and Hamilton, J. L. (2018). Potential for
904 offsetting diamond mine carbon emissions through mineral carbonation of processed kimberlite: an assessment
905 of De Beers mine sites in South Africa and Canada. Mineral. Petrol. 112, 755-765. doi: 10.1007/s00710-018-
906 0589-4

907 Meyer, N. A., Vogeli, J. U., Becker, M., Broadhurst, J. L., Reid, D. L., and Franzidis, J.-P. (2014). Mineral carbonation
908 of PGM mine tailings for CO_2 storage in South Africa: a case study. Mineral. Eng. 59, 45-51. doi:
909 10.1016/j.mineng.2013.10.014

910 Mining Association of Canada, (2014). Towards sustainable mining. Progress Report, mining.ca/towards-
911 sustainable-mining, 159 pp.

912 Morse, J.W., Arvidson, R.S., and Luttge, A. (2007). Calcium carbonate formation and dissolution. Chem. Rev.,
913 107, (2), 342-81. doi: 10.1021/cr050358j

914 Myers, C., and Nakagaki, T., (2020). Direct mineralization of atmospheric CO_2 using natural rocks in Japan.
915 Environ. Res. Lett. 15, 124018. doi: 10.1088/1748-9326/abc217

916 National Academies of Sciences, Engineering, and Medicine (NASEM) (2019). Negative Emissions Technologies
917 and Reliable Sequestration: A Research Agenda. Washington DC: The National Academies Press. NPR, 2021

918 Ndlovu, S., Simate, G. S., and Matinde, E. (2017). Waste Production and Utilization in the Metal Extraction
919 Industry. Boca Raton: CRC Press, Taylor and Francis Group.

920 Oelkers E.H. (2001). General kinetic description of multioxide silicate mineral and glass dissolution. Geochim.
921 Cosmochim. Acta 65, 3703–3719. doi: 10.1016/S0016-7037(01)00710-4

922 O'Neil, J.R., and Barnes, I. (1971). C^{13} and O^{18} compositions in some fresh-water carbonates associated with
923 ultramafic rocks and serpentinites: western United States. Geochim. Cosmochim. Acta, 35, 687-697. doi:
924 10.1016/0016-7037(71)90067-6

925 Oskierski, H.C., Dlugogorski, B.Z., and Jacobsen, G., (2013). Sequestration of atmospheric CO_2 in a weathering-
926 derived, serpentinite-hosted magnesite deposit: ^{14}C tracing of carbon sources and age constraints for a refined
927 genetic model. Geochim. Cosmochim. Acta 122, 225-146. doi: 10.1016/j.gca.2013.08.029

928 Palandri, J. L., and Kharaka, Y. K. (2004). A Compilation of Rate Parameters of Water-Mineral Interaction Kinetics
929 for Application to Geochemical Modelling. U.S. Geological Survey Open File Report 2004-1068.

930 Pokrovsky, O.S., and Schott, J., (2000). Kinetics and mechanism of forsterite dissolution at 25°C and pH from 1
931 to 12. Geochim. Cosmochim. Acta 64, 3313–3325. doi: 10.1016/S0016-7037(00)00434-8

Power, I. M., Dipple, G. M., Bradshaw, P. M. D., and Harrison, A. L. (2020). Prospects for CO_2 mineralization and enhanced weathering of ultramafic mine tailings from the Baptise nickel deposit in British Columbia, Canada. Int. J. Greenhouse Gas Control 94:102895. doi: 10.1016/j.ijggc.2019.102895

Power, I. M., Harrison, A. L., and Dipple, G. M. (2016). Accelerating mineral carbonation using carbonic anhydrase. Environ. Sci. Technol. 50, 2610-2618. doi: 10.1021/acs.est.5b04779

Power, I. M., Harrison, A. L., Dipple, G. M., and Southam, G. (2013). Carbon sequestration via carbonic anhydrase facilitated magnesium carbonate precipitation. Int. J. Greenhouse Gas Control 16, 145-155. doi: 10.1016/j.ijggc.2013.03.011

Power, I. M., McCutcheon, J., Harrison, A. L., Wilson, S. A., Dipple, G. M., Kelly, S., et al. (2014). Strategizing carbon-neutral mines: a case for pilot projects. Minerals 4, 399-436. doi: 10.3390/min4020399

Pronost, J., Beaudoin, G., Tremblay, J., Larachi, F., Duchesne, J., Hébert, R., et al. (2011). Carbon sequestration kinetic and storage capacity of ultramafic mining waste. Environ. Sci. Technol. 45, 9413-9420. doi: 10.1021/es203063a

Pu, Y., Li, L., Wang, Q., Shi, X., Fu, L., Zhang, G., Luan, C. and El-Fatah Abomohra, A. (2021). Accelerated carbonation treatment of recycled concrete aggregates using flue gas: A comparative study towards performance improvement. Journal of CO2 Utilization 43, 101362. doi: 10.1016/j.jcou.2020.101362

Renforth, P. (2019). The negative emission potential of alkaline materials. Nat. Commun. 10:1401. doi: 10.1038/s41467-019-09475-5

Renforth, P., (2012). The potential of enhanced weathering in the UK. Int. J. Greenhouse Gas Control 10, 229-243. doi: 10.1016/j.ijggc.2012.06.011

Renforth, P., and Henderson, G. (2017). Assessing ocean alkalinity for carbon sequestration. Rev. Geophys. 55, 636-674. doi: 10.1002/2016RG000533

Renforth, P., Pogge von Strandmann, P.A.E., and Henderson, G.M. (2015). The dissolution of olivine added to soil: Implications for enhanced weathering. Appl. Geochem., 61, 109-118. doi: 10.1016/j.apgeochem.2015.05.016

957 Rigopoulos, I., Vasiliades, M.A., Petallidou, K.C., Ioannou, I., Efstathiou, A.M., and Kyratsi, T., (2015). A method
958 to enhance the CO_2 storage capacity of pyroxenitic rocks. Greenh. Gas. Sci. Technol. 5, 1-14. doi:
959 10.1002/ghg.1502.

960 Saldi, G.D., Jordan, G., Schott, J., and Oelkers E.H. (2009). Magnesite growth rates as function of temperature
961 and saturation state Geochim. Cosmochim. Acta, 73, 5646-5657. doi: 10.1016/j.gca.2009.06.035

962 Saldi, G.D., Schott, J., Pokrovsky, O.S., and Oelkers, E.H. (2010). An experimental study of magnesite dissolution
963 rates at neutral to alkaline conditions at 150 and 200 °C as a function of pH, total dissolved carbonate
964 concentration and chemical affinity. Geochim. Cosmochim. Acta, 74, 6344-6356. doi: 10.1016/j.gca.2010.07.012

965 Saldi, G.D., Schott, J., Pokrovsky, O.S., Gautier, Q., and Oelkers, E.H. (2012). An experimental study of magnesite
966 precipitation rates at neutral to alkaline conditions and 100–200 °C as a function of pH, aqueous solution
967 composition and chemical affinity. Geochim. Cosmochim. Acta, 83, 93-109. doi: 10.1016/j.gca.2011.12.005

968 Salek, S. S., Kleerebezem, R., Jonkers, H. M., Witkamp, G.-J. and van Loosdrecht, M. C.M. (2013). Mineral CO_2
969 sequestration by environmental biotechnological processes. Trends Biotechnol. 31, 139-146. doi:
970 10.1016/j.tibtech.2013.01.005

971 Schott, J., Pokrovsky, O. S., and Oelkers, E. H. (2009). The link between mineral dissolution/precipitation kinetics
972 and solution chemistry. Rev. Mineral. Geochem. 70, 207–258. doi:10.2138/rmg.2009.70.6

973 Schuiling, R. D., and Krijgsman, P. (2006). Enhanced weathering: an effective and cheap tool to sequester CO_2.
974 Clim. Change 74, 349-354. doi: 10.1007/s10584-005-3485-y

975 Schuiling, R.D., and de Boer, P.L., (2011). Rolling stones; fast weathering of olivine in shallow seas for cost-
976 effective CO_2 capture and mitigation of global warming and ocean acidification. Earth Syst. Dynam. Discuss. 2,
977 551-568. doi: 10.5194/esdd-2-551-2011

978 Sipilä, S., Teir, S., and Zevenhoven, R. (2008). Sequestration by Mineral Carbonation, Literature Review Update
979 2005-2007. Report VT 2008-1. Turku: Åbo Akademi University Faculty of Technology Heat Engineering
980 Laboratory.

981 Steinour, H. H. (1959). Some effects of carbon dioxide on mortars and concrete-discussion. J. Am. Concr. 30,
982 905–907.

ten Berge, H. F. M., van der Meer, H. G., Steenhuizen, J. W., Goedhart, P. W., Knops, P., and Verhagen, J. (2012). Olivine weathering in soil, and its effects on growth and nutrient uptake in ryegrass (*Lolium perenne* L.): a pot experiment. PLoS ONE 7:e42098. doi: 10.1371/journal.pone.0042098

United Nations Environment Programme (UNEP) (2017). The Emissions Gap Report 2017. Nairobi: UNEP.

United States Geological Survey (USGS) (2021). Mineral Commodity Summaries 2021. Reston, VA: U.S. Geological Survey.

Vogeli, J., Reid, D. L., Becker, M., Broadhurst, J., and Franzidis, J.-P. (2011). Investigation of the potential for mineral carbonation of PGM tailings in South Africa. Miner. Eng. 24, 1348-1356. doi: 10.1016/j.mineng.2011.07.005

Wang, D., Xiong, C., Li, W., and Chang, J., (2020). Growth of calcium carbonate induced by accelerated carbonation of tricalcium silicate. ACS Sustainable Chem. Eng., 8, 14718-14731. doi: 10.1021/acssuschemeng.0c02260

Wang, Z., and Giammar, D.E., (2003). Mass action expressions for bidentate adsorption in surface complexation modeling: theory and practice, Environ. Sci. Technol., 47, 3982-3996. doi: 10.1021/es305180e

Wilcox, J., Kolosz, B., and Freeman, J. (2021). CDR Primer. Available online at: https://cdrprimer.org/ (accessed March 1, 2021).

Wilson, S. A., Dipple, G.M., Power, I.M., Thom, J.M., Anderson, R. G., Raudsepp, M., et al. (2009a). Carbon dioxide fixation within mine wastes of ultramafic hosted ore deposits: examples from the Clinton Creek and Cassiar chrysotile deposits, Canada. Econ. Geol. 104, 95-112. doi: 10.2113/gsecongeo.104.1.95

Wilson, S. A., Harrison, A. L., Dipple, G. M., Power, I. M., Barker, S. L. L., Mayer, K. U., et al. (2014). Offsetting of CO_2 emissions by air capture in mine tailings at the Mount Keith Nickel Mine, Western Australia: rates, controls and prospects for carbon neutral mining. Int. J. Greenh. Gas Con. 25, 121-140. doi: 10.1016/j.ijggc.2014.04.002

Wilson, S.A., Barker, S.L.L., Dipple, G.M., and Atudorei, V., (2010). Isotopic disequilibrium during uptake of atmospheric CO_2 into mine process waters: implications for CO_2 sequestration. Environ. Sci. Technol. 44, 9522-9529. doi: 10.1021/es1021125

Wilson, S.A., Raudsepp, M., and Dipple, G.M., (2009b). Quantifying carbon fixation in trace minerals from processed kimberlite: A comparative study of quantitative methods using X-ray powder diffraction data with applications to the Diavik Diamond Mine, Northwest Territories, Canada. Appl. Geochem. 24, 2312-2331. doi: 10.1016/j.apgeochem.2009.09.018

Wogelius, R.A., and Walther, J.V., (1992). Olivine dissolution kinetics at near-surface conditions. Chem. Geol., 97, 1-2, 101-112. doi: 10.1016/0009-2541(92)90138-U

Xing, L., Darton, R. C., and Yang, A. (2021). Enhanced weathering to capture atmospheric carbon dioxide: Modeling of a trickle-bed reactor. AIChE J. 67:e17202. doi: 10.1002/aic.17202

Zarandi, A.E., Larachi, F., Beaudoin, G., Plante, B., and Sciortino, M. Multivariate study of the dynamics of CO_2 reaction with brucite-rich ultramafic mine tailings. Int. J. Greenhouse Gas Control 52, 110-119. doi: 10.1016/j.ijggc.2016.06.022

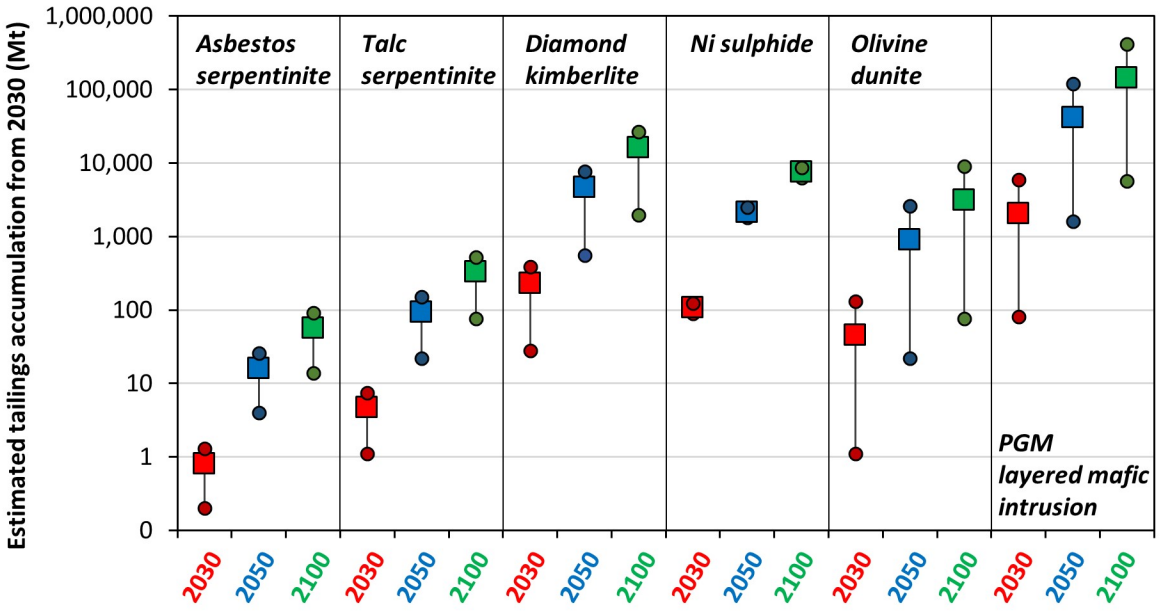
Estimated tailings accumulation from 2030 (Mt)
1,000,000
100,000
10,000
1,000
100
10
1
0
Asbestos serpentinite
Talc serpentinite
Diamond kimberlite
Ni sulphide
Olivine dunite
PGM layered mafic intrusion
2030
2050
2100

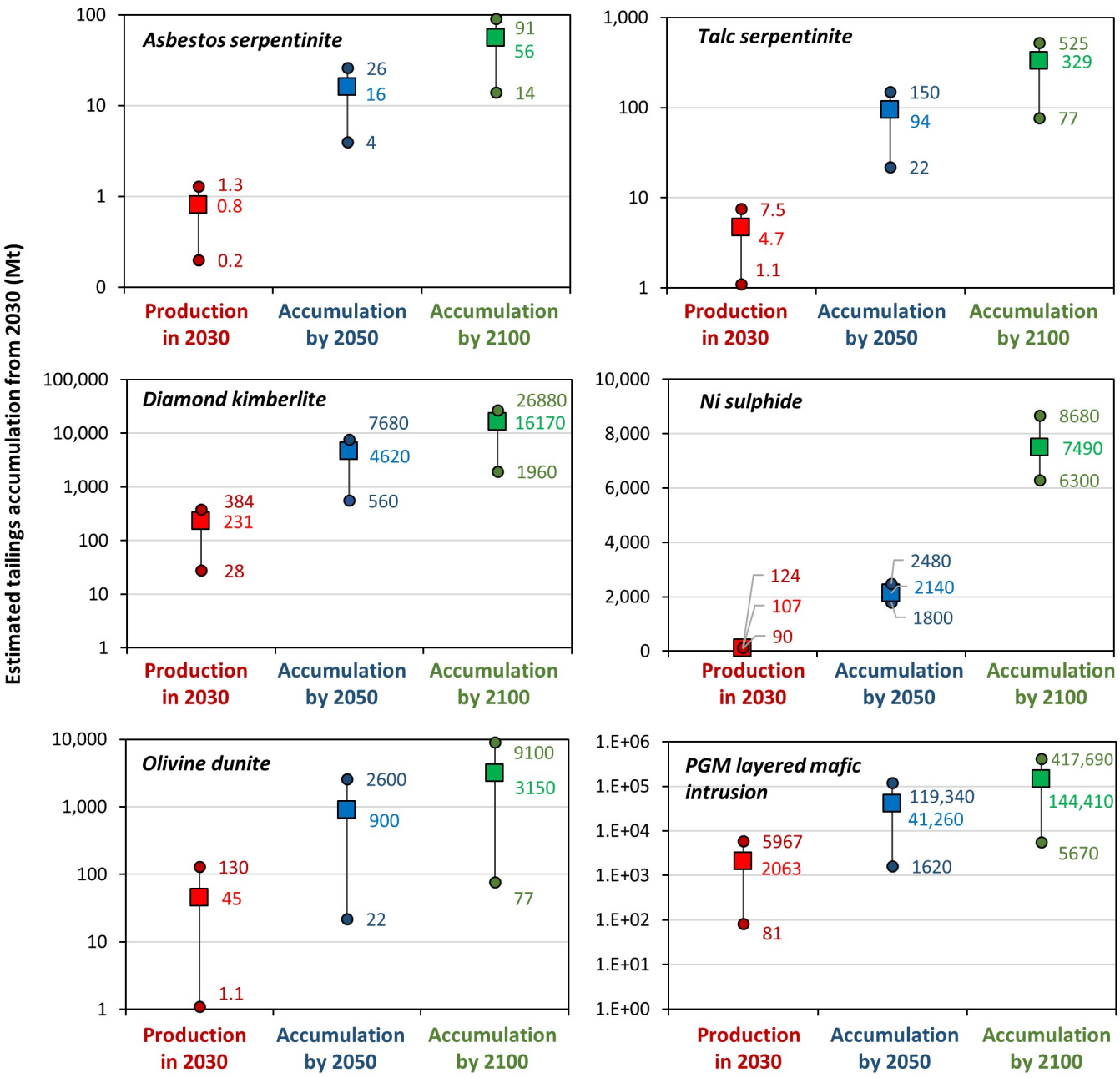
Estimated tailings accumulation from 2030 (Mt)
Asbestos serpentinite
1.3
0.8
0.2
26
16
4
91
56
14
Talc serpentinite
7.5
4.7
1.1
150
94
22
525
329
77
Diamond kimberlite
384
231
28
7680
4620
560
26880
16170
1960
Ni sulphide
124
107
90
2480
2140
1800
8680
7490
6300
Olivine dunite
130
45
1.1
2600
900
22
9100
3150
77
PGM layered mafic intrusion
5967
2063
81
119,340
41,260
1620
417,690
144,410
5670
Production in 2030
Accumulation by 2050
Accumulation by 2100

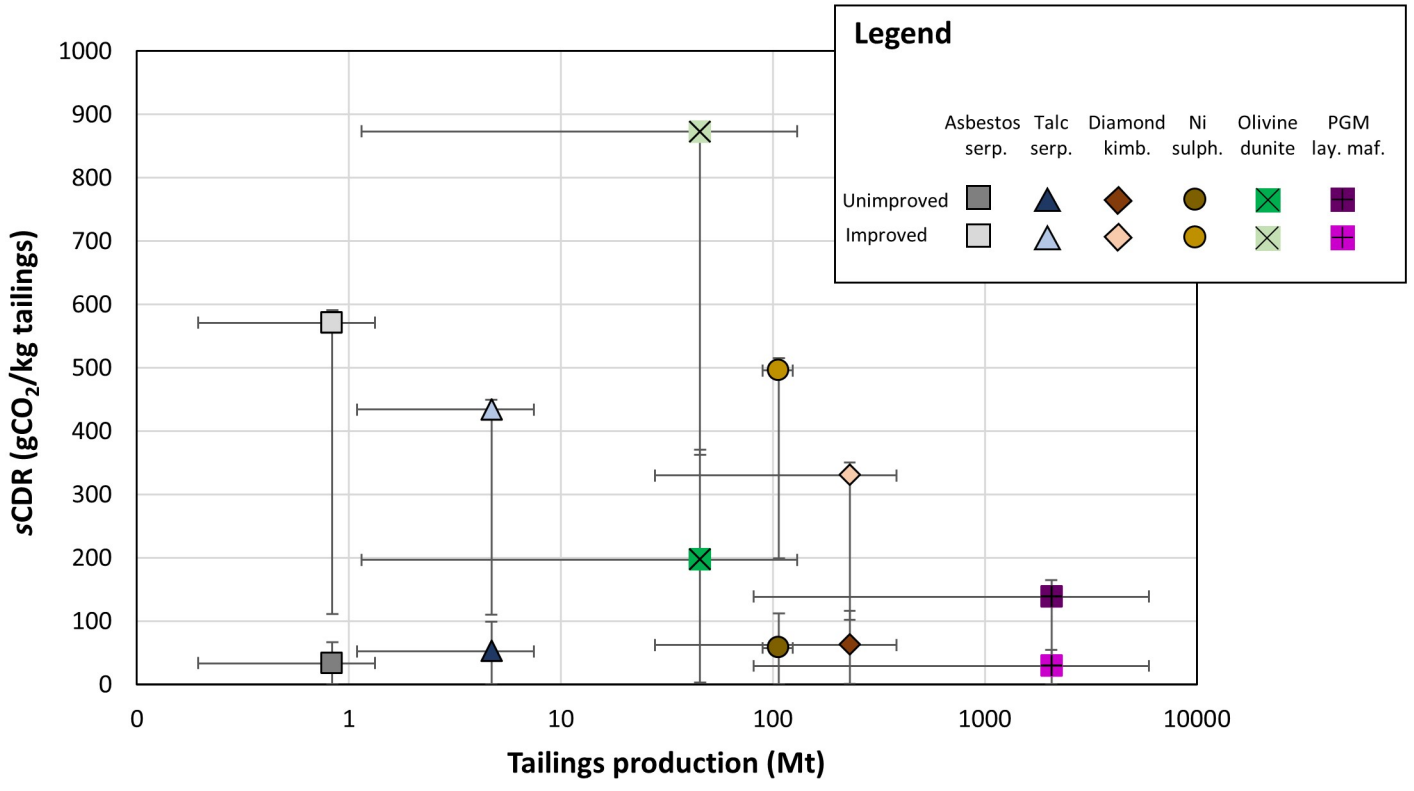
Legend
Asbestos serp.
Talc serp.
Diamond kimb.
Ni sulph.
Olivine dunite
PGM lay. maf.
Unimproved
Improved
sCDR (gCO2/kg tailings)
Tailings production (Mt)
0
100
200
300
400
500
600
700
800
900
1000
0
1
10
100
1000
10000

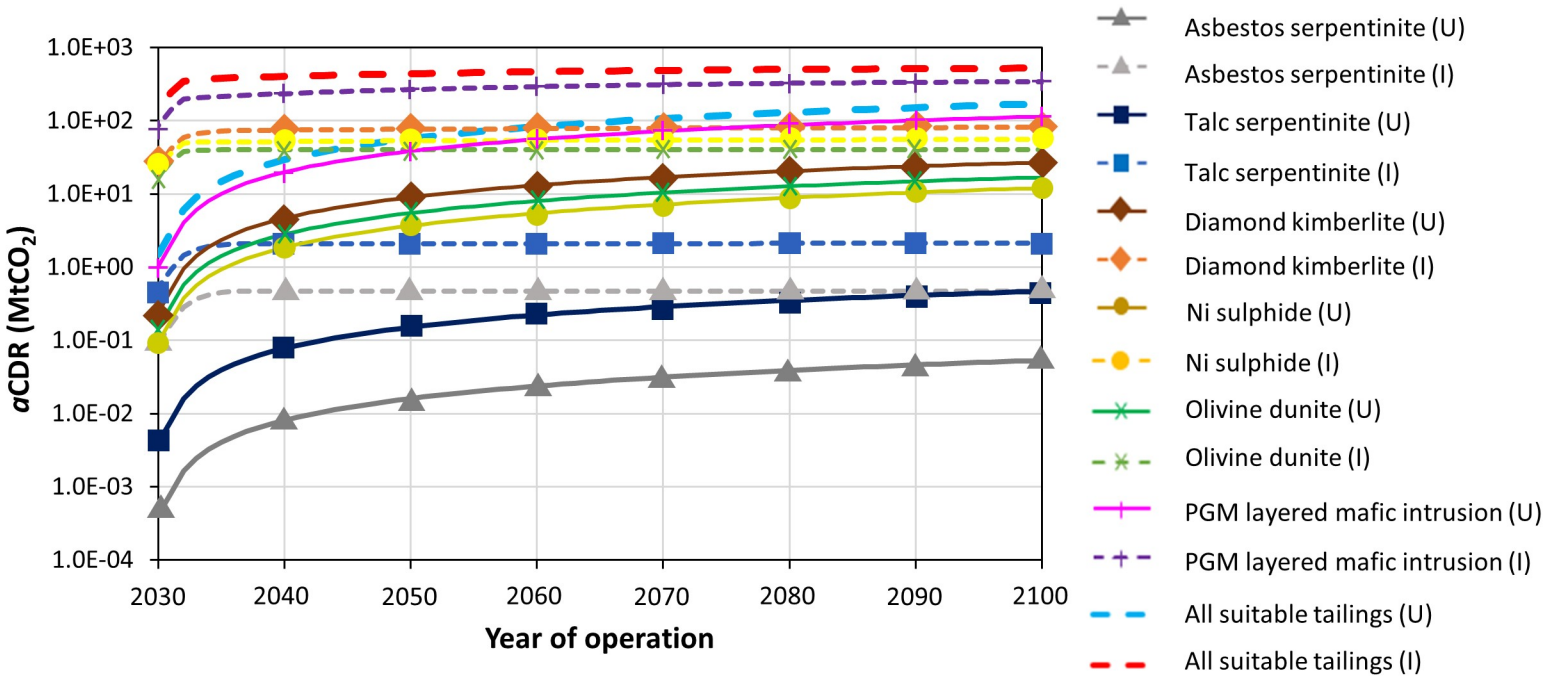
1.0E+03
1.0E+02
1.0E+01
1.0E+00
1.0E-01
1.0E-02
1.0E-03
1.0E-04
αCDR (MtCO2)
2030
2040
2050
2060
2070
2080
2090
2100
Year of operation
Asbestos serpentinite (U)
Asbestos serpentinite (I)
Talc serpentinite (U)
Talc serpentinite (I)
Diamond kimberlite (U)
Diamond kimberlite (I)
Ni sulphide (U)
Ni sulphide (I)
Olivine dunite (U)
Olivine dunite (I)
PGM layered mafic intrusion (U)
PGM layered mafic intrusion (I)
All suitable tailings (U)
All suitable tailings (I)

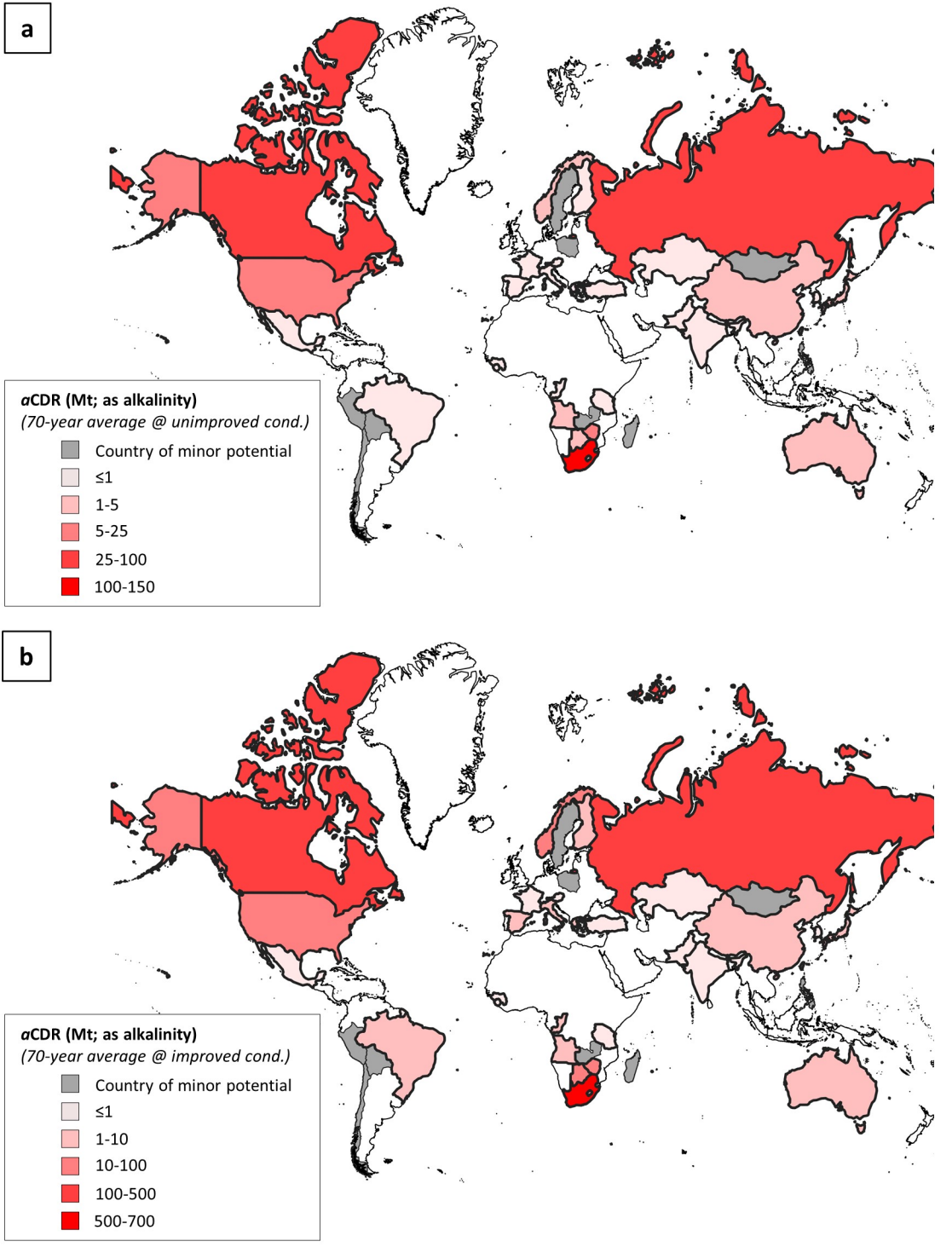
a
aCDR (Mt; as alkalinity)
(70-year average @ unimproved cond.)
Country of minor potential
≤1
1-5
5-25
25-100
100-150
b
aCDR (Mt; as alkalinity)
(70-year average @ improved cond.)
Country of minor potential
≤1
1-10
10-100
100-500
500-700

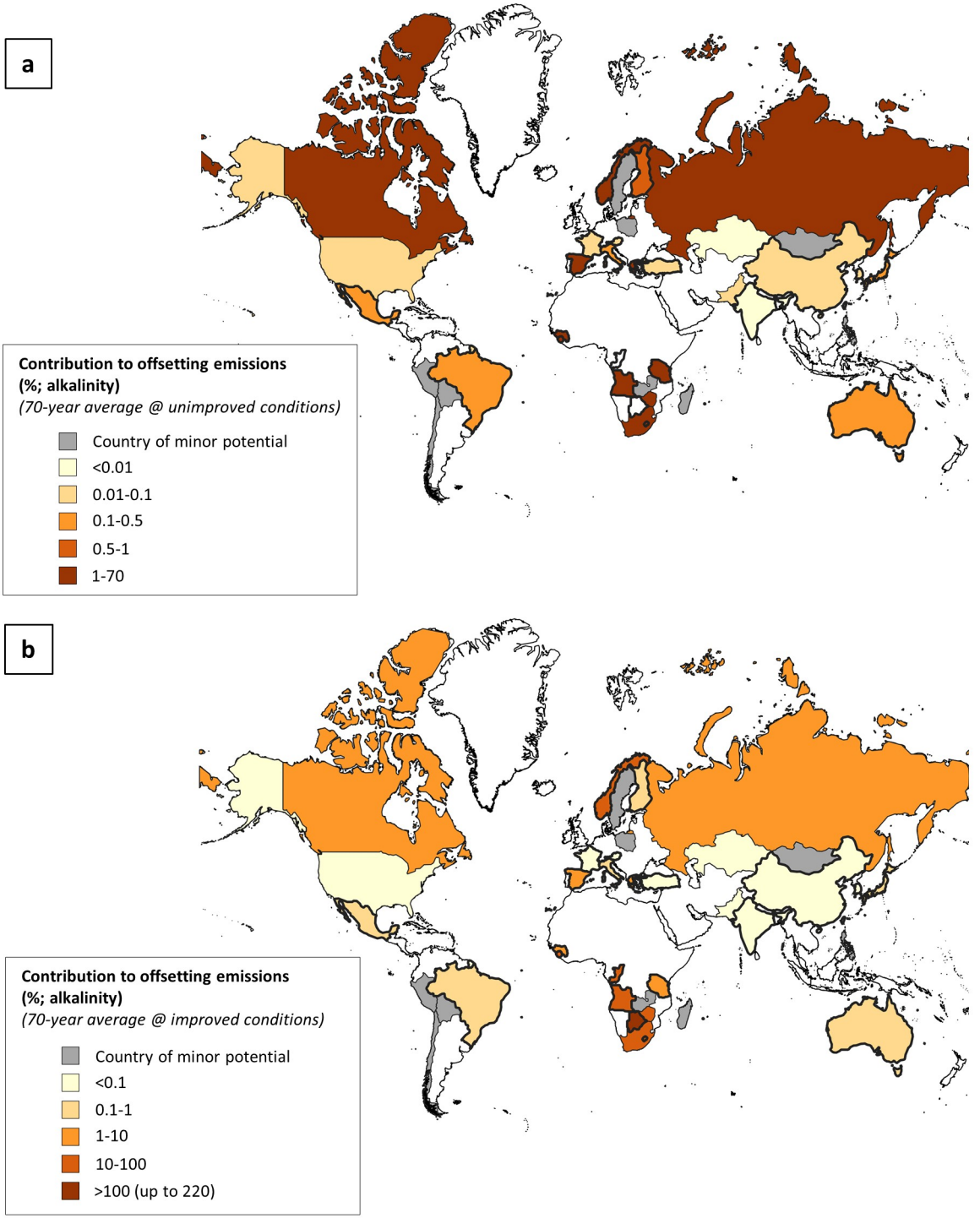
a
Contribution to offsetting emissions
(%; alkalinity)
(70-year average @ unimproved conditions)
Country of minor potential
<0.01
0.01-0.1
0.1-0.5
0.5-1
1-70
b
Contribution to offsetting emissions
(%; alkalinity)
(70-year average @ improved conditions)
Country of minor potential
<0.1
0.1-1
1-10
10-100
>100 (up to 220)

Table 1. List of selected silicate-hosted mine tailings (classified by their targeted commodity and typical host rock) for initial assessment of CDR potential (after Bullock et al., 2021).

Targeted commodity	General host rock deposit type
Aluminium (Al)	Bauxite
Asbestos	Serpentinite
Gold (Au)	Carlin-type
Au	Orogenic
Au-silver (Ag)	Hydrothermal
Chrome (Cr)	Layered mafic intrusion
Cr	Podiform
Copper (Cu)	Iron oxide copper gold (IOGC)
Cu	Porphyry
Cu	Sediment-hosted
Cu	Volcanogenic massive sulphide (VMS)
Diamond	Alluvial
Diamond	Kimberlite
Iron (Fe)	Banded iron formation (BIF)
Fe	Ironstone
Fe	Kiruna-type
Nickel (Ni)	Laterite
Ni	Sulphide
Olivine (refractory mineral for slag conditioning)	Dunite
Lead-zinc (Pb-Zn)	Sedimentary exhalative (SEDEX)
Pb-Zn	Skarn
Platinum group metals (PGM)	Layered mafic intrusion
Tin (Sn)	Granite-related
Sn	Secondary
Talc	Serpentinite
Titanium (Ti)	Mafic-associated (anorthosite)
Uranium (U)	Hematite breccia complex
U	Metasomatic
U	Quartz pebble conglomerates
Tungsten (W)	Shale
W	Wolframite vein

Table 2. Typical targetable minerals (selected based on their favourable Ca-Mg content and mineral E_{pot}) found in the assessed tailings deposits, and their kinetic properties. Dissolution rates (W_r) include published rates achieved under "unimproved" (near-neutral) conditions ("Neut" - mean values of published experimental W_r achieved at solution pH 6-8, temperature 21-24°C, ambient pCO_2) or under any applied reaction conditions ("any").

Mineral Group	General chemical formula	Mean mineral E_{pot} (gCO_2/kg)	Mean W_r at near-neutral(^{Neutr}) conditions (log mol/m^2/s)	Max W_r^{Neut} (log mol/m^2/s) W_r^{Neut}	Min (log mol/m^2/s) W_r^{Neut}	Fastest rate for any applied conditions (W_r^{any}; log mol/m^2/s)	pH (W_r^{any})	Temp (°C) (W_r^{any})
Hornblende	$Ca_2(Mg,Fe,Al)_5(Si,Al)_8O_{22}(OH)_2$	482	-12.51	-11.73	-13.0	-9.91	1.6	~24
Biotite	$K(Mg,Fe)_3(AlSi_3O_{10})(F,OH)_2$	457	-12.07	-11.9	-12.24	-10.3	1.1	~22
Clinochlore	$Mg_5Al(AlSi_3O_{10})(OH)_8$	416	-12.52	-	-	-12.52	4.5	~24
Clinopyroxene	$(Ca,Mg,Fe,Na)(Mg,Fe,Al)(Si,Al)_2O_6$	443	-11.12	-10.8	-12.4	-8.1	1.5	~22
Forsterite	Mg_2SiO_4	938	-10.04	-9.6	-10.57	-6.09	2.0	~64
Orthopyroxene	$(Fe,Mg)_2Si_2O_6$	479	-11.63	-11.0	-12.5	-9.1	1.6	~24
Plagioclase	$(Na,Ca)(Si,Al)_4O_8$	179	-11.60	-9.58	-14.61	-5.1	1.3	~300
Serpentine	$Mg_6Si_4O_{10}(OH)_8$	624	-11.60	-9.79	-12.4	-5.7	0.0	~24
Talc	$Mg_3Si_4O_{10}(OH)_2$	522	-12.00	-	-	-12.0	4.5	~24
Wollastonite	$CaSiO_3$	568	-9.80	-8.0	-11.6	-8.0	7.2	~24

Dissolution rates at near-neutral conditions (W_r^{Neut} = pH 6-8, 21-24°C and atmospheric CO_2, based on Si release rate) presented from average or single point data taken from compilations by Palandri and Kharaka (2004), Bandstra et al. (2008) and others (see Supplementary Material B). Mineral groups and associated calculated W_r values represent average of presented end member compositions, with the exceptions of amphibole (hornblende only), mica (biotite only), chlorite (clinochlore only), olivine (forsterite only), clay (talc only) and inosilicate (wollastonite only); see Table 2. End members selected based on chemical favourability (containing divalent Mg and Ca cations) and availability of data. Max and Min W_r^{Neut} presented to highlight effects of variations in mineral chemistry and end member compositions; see Table 2. See Supplementary Material B for detailed information on W_r sources.

Table 3. Estimates of dissolution extent over time (on decadal timescales of up to 70 years) for a theoretical 1 kg of tailings material at typical grain sizes (Table 1) and unimproved conditions (using W_r^{Neut}; see Tables 1-2 and Supplementary Material B). Assessment undertaken to aid determination of most suitable tailings materials for CDR purposes for tailings deemed potentially chemically favourable (see text). Calculated *s*CDR potential over 70 years also shown as gCO_2 removed as alkalinity. Maximum and minimum values shown in brackets to account for variations in W_r^{Neut} (Tables 1-2). Minerals present and estimated modal content of tailings based on information presented in Table 3, with unwanted minerals (e.g., sulphides, Fe oxides) not listed (though their weighted contribution to theoretical 1 kg of material has been factored in to calculations).

Tailings material	**Mineral**	**Dissolution (%) after 1 year**	**Dissolution (%) after 70 years**	**Time for complete mineral dissolution (years)**	***s*CDR for mineral in 1 kg of tailings after 70 years (gCO_2/kg)**
Asbestos serpentinite	Olivine	1.0 (0.3-2.8)	54.7 (19.2-95.3)	298 (108-1009)	10.3 (3.6-17.9)
Typical grain size = 75 µm	Serpentine	0.2 (0.02-9.3)	9.9 (1.6-100*)	2023 (31-12766)	56.2 (9.2-568*)
	Clinopyroxene	0.1 (0.003-0.06)	4.3 (0.2-8.9)	4744 (2270-90390)	0.2 (0.01-0.4)
					TOTAL = 66.6 (12.8-587.0)
Cr layered intrusion	Orthopyroxene	0.003 (4E-4-0.04)	0.2 (0.03-0.8)	108124 (25347-801534)	0.3 (0.04-1.4)
Typical grain size = 250 µm	Clinopyroxene	0.02 (0.001-0.02)	1.3 (0.07-2.7)	15812 (7568-301299)	0.4 (0.02-0.8)
					TOTAL = 0.7 (0.07-2.3)
Cr podiform	Olivine	0.3 (0.09-0.8)	19.5 (6.0-47.2)	992 (360-3363)	76.7 (23.8-185.8)
Typical grain size = 250 µm	Clinopyroxene	0.02 (0.001-0.04)	1.3 (0.07-2.7)	15812 (7568-301299)	0.8 (0.04-1.7)
					TOTAL = 56.4 (23.8-187.5)
Cu porphyry	Amphibole	0.002 (0.001-0.01)	0.1 (0.03-0.7)	183172 (30399-566057)	0.05 (0.02-0.3)
Typical grain size = 120 µm	Orthopyroxene	0.006 (0.001-0.02)	0.4 (0.05-1.7)	51900 (12166-384737)	0.3 (0.04-1.2)
	Plagioclase	0.01 (9.7E-06-1.0)	0.7 (7E-4-56.2)	30060 (287-30760061)	0.4 (1.4E-4-30.2)
	Clinopyroxene	0.04 (0.002-0.1)	2.7 (0.17-5.6)	7590 (3633-144624)	1.8 (0.1-3.7)
	Biotite	0.007 (0.005-0.01)	0.5 (0.3-0.7)	43455 (29379-64275)	0.2 (0.07-0.3)
					TOTAL = 2.7 (0.3-35.8)

Cu VMS	Amphibole	0.002 (1.6E-4-0.01)	0.1 (0.04-0.8)	152644 (25333-471714)	0.1 (0.04-0.8)
Typical grain size = 100 µm	Orthopyroxene	0.007 (1.9E-4-0.03)	0.5 (0.06-2.0)	43250 (10139-320614)	0.05 (0.01-0.2)
	Plagioclase	0.01 (1.2E-05-1.3)	0.8 (0.001-64.0)	25050 (239-25633384)	0.4 (1.4E-4-34.4)
	Clinopyroxene	0.05 (0.002-0.1)	3.2 (0.2-6.7)	6325 (3027-120520)	0.4 (0.02-0.9)
	Biotite	0.008 (0.006-0.01)	0.6 (0.4-0.8)	36213 (24483-53563)	0.4 (0.3-0.6)
	Chlorite	0.004	0.3	74059	0.1
					TOTAL = 1.6 (0.5-36.9)
Diamond kimberlite	Olivine	1.0 (0.3-2.8)	54.7 (19.2-95.3)	298 (108-1009)	102.6 (35.9-179)
Typical grain size = 75 µm	Orthopyroxene	0.01 (0.001-0.04)	0.6 (0.09-2.7)	32437 (7604-240460)	0.2 (0.02-0.7)
	Serpentine	0.2 (0.02-9.3)	9.9 (1.6-100*)	2023 (31-12766)	12.3 (2.0-124.8*)
	Clinopyroxene	0.1 (0.003-0.1)	4.3 (0.2-8.9)	4744 (2270-90390)	1.0 (0.05-2.0)
	Biotite	0.01 (0.007-0.02)	0.8 (0.5-1.1)	27160 (18362-40172)	0.7 (0.5-1.0)
					TOTAL = 116.7 (38.5-307.2)
Ni sulphide	Olivine	0.4 (0.11-1.0)	23.9 (7.5-56.0)	794 (288-2690)	112.0 (35.2-262.7)
Typical grain size = 200 µm	Orthopyroxene	0.003 (5E-4-0.01)	0.2 (0.03-1.0)	86499 (20277-641228)	0.1 (0.02-0.5)
	Clinopyroxene	0.02 (0.001-0.05)	1.6 (0.1-3.4)	12650 (6055-241039)	0.7 (0.04-1.5)
					TOTAL = 112.9 (35.2-264.7)
Olivine dunite	Olivine	0.8 (0.22-2.1)	43.6 (14.6-86)	397 (144-1345)	368.3 (123.4-724.8)
Typical grain size = 100 µm	Orthopyroxene	0.007 (9E-4-0.03)	0.5 (0.06-2.0)	43250 (10139-320614)	0.05 (0.01-0.2)
	Clinopyroxene	0.05 (0.002-0.1)	3.2 (0.2-6.7)	6325 (3027-120520)	0.4 (0.02-0.9)
	Serpentine	0.1 (0.02-7.0)	7.5 (1.2-100*)	2698 (42-17022)	2.3 (0.4-31.2*)
					TOTAL = 371.1 (123.8-757.1)
Pb-Zn skarn	Amphibole	0.001 (3E-4-0.005)	0.1 (0.04-0.8)	152644 (25333-471714)	0.07 (0.02-0.4)
Typical grain size = 100 µm	Plagioclase	0.005 (5E-06-0.6)	0.8 (0.001-64.0)	25050 (239-25633384)	0.2 (1.4E-4-11.5)
	Biotite	0.004 (0.003-0.006)	0.6 (0.4-0.8)	36213 (24483-53563)	0.3 (0.2-0.4)

					TOTAL = 0.5 (0.2-12.23)
PGM layered mafic intrusion	Olivine	1.0 (0.3-2.8)	54.7 (19.2-95.3)	298 (108-1009)	51.3 (17.97-89.4)
Typical grain size = 75 µm	Orthopyroxene	0.01 (0.001-0.04)	0.6 (0.09-2.7)	32437 (7604-240460)	1.5 (0.2-6.5)
	Plagioclase	0.02 (2E-5-1.7)	1.1 (0.001-76.7)	18787 (179-19225038)	0.3 (3E-4-20.6)
	Clinopyroxene	0.1 (0.003-0.1)	4.3 (0.2-8.9)	4744 (2270-90390)	1.9 (0.1-3.9)
	Biotite	0.01 (0.007-0.02)	0.8 (0.5-1.1)	27160 (18362-40172)	0.2 (0.003-0.3)
					TOTAL = 55.2 (18.3-120.6)
Talc serpentinite	Serpentine	0.2 (0.02-9.3)	9.9 (1.6-100*)	2023 (31-12766)	31.7 (5.2-330.7*)
Typical grain size = 75 µm	Olivine	1.0 (0.3-2.8)	54.7 (19.2-95.3)	298 (108-1009)	66.7 (23.4-116.2)
	Chlorite	0.01	0.4	55544	0.3
	Talc	0.01	0.8	26182	0.5
	Amphibole	0.003 (8E-4-0.02)	0.2 (0.06-1.1)	116444 (19325-359848)	0.02 (0.01-0.1)
					TOTAL = 99.3 (29.4-447.9)
Ti anorthosite	Plagioclase	0.006 (5.9E-06-0.6)	0.4 (4E-4-37.3)	50100 (478-51266768)	0.4 (3.6E-4-33.4)
Typical grain size = 200 µm	Orthopyroxene	0.003 (4.7E-4-0.01)	0.2 (0.03-1.0)	86499 (20277-641228)	0.2 (0.03-1.0)
	Olivine	0.4 (0.11-1.0)	23.9 (7.5-56.0)	794 (2690-288)	22.4 (7.5-52.5)
					TOTAL = 23.0 (7.1-86.9)

*Full dissolution of mineral (total grams available in 1 kg of a given tailings) achieved before 70 years. For shrinking core model used here (after Renforth et al., 2015), molar volume of mineral converted to one mol Si basis.

Table 4. Total cumulative CDR (*t*CDR; $MtCO_2$ as alkalinity) based on annual tailings production estimates, and average $E_{pot}^{op,i}$ of 1 kg of suitable tailings (CO_2 removed as alkalinity) after 1-70 years of operation, both under unimproved and improved reaction conditions (from implementation in 2030 onwards). Calculated values are based on mean annual and mean cumulative production estimates from Table 3.

		***t*CDR ($MtCO_2$) within a given period**			**$E_{pot}^{op,i}$ ($kgCO_2/kg$) for a given period of weathering (years)**		
Type of tailings	**Applied conditions**	**2030-2031**	**2030-2050**	**2030-2100**	**2030-2031**	**2030-2050**	**2030-2100**
Asbestos serpentinite	Unimproved	<0.01	0.2	2	5.1E-04	0.01	0.04
	Improved	0.1	9	33	0.12	0.56	0.59
Talc serpentinite	Unimproved	<0.01	1	18	8.5E-04	0.01	0.05
	Improved	0.5	38	145	0.11	0.4	0.44
Diamond kimberlite	Unimproved	0.2	88	1029	9.0E-04	0.02	0.06
	Improved	24	1379	5407	0.1	0.3	0.33
Ni sulphide	Unimproved	0.1	35	441	9.4E-04	0.02	0.06
	Improved	21	986	3761	0.2	0.46	0.5
Olivine dunite	Unimproved	0.1	53	635	2.2E-03	0.06	0.2
	Improved	17	761	2815	0.37	0.84	0.89
PGM layered mafic intrusion	Unimproved	1.0	373	4365	4.9E-04	0.01	0.03
	Improved	84	4437	20351	0.04	0.11	0.14
TOTAL (tCDR)	**Unimproved**	**1.4**	**550**	**6490**			
	Improved	**147**	**7610**	**32512**			